

NAFION MODIFIED NCA CATHODE SYNTHESIS FOR SUPERIOR CYCLING  
PERFORMANCE OF LITHIUM-ION BATTERIES

by  
AYÇA YİĞİTALP

Submitted to the Graduate School of Engineering and Natural Sciences  
In partial fulfillment of the requirements for the degree of  
Master of Science

Sabancı University  
July 2019

NAFION MODIFIED NCA CATHODE SYNTHESIS FOR SUPERIOR  
CYCLING PERFORMANCE OF LITHIUM-ION BATTERIES

APPROVED BY:

Prof. Dr. Selmiye Alkan Gürsel  
(Thesis Supervisor)



Asst. Prof. Dr. Alp Yürüm  
(Thesis Co-Advisor)



Asst. Prof. Dr. Burcu Dedeoğlu  
(Gebze Technical University)



Assoc. Prof. Dr. Emre Erdem



Asst. Prof. Dr. Mustafa Kemal Bayazit



DATE OF APPROVAL: 19/07/2019

©AYÇA YİĞİTALP  
All Rights Reserved

NAFION MODIFIED NCA CATHODE SYNTHESIS FOR SUPERIOR CYCLING  
PERFORMANCE OF LITHIUM-ION BATTERIES

AYÇA YİĞİTALP

Material Science and Nano Engineering, M.Sc. Thesis, July 2019

Thesis supervisors:

Prof. Dr. Selmiye Alkan Gürsel

Asst. Prof. Dr. Alp Yürüm (Co-Supervisor)

**Place: SUNUM**

**Keywords:** Lithium-ion batteries, NCA cathode, energy applications, surface modification of cathode, NCA

**ABSTRACT**

Lithium-ion batteries, due to their high energy density and portable dimensions, play a very important role in today's technology. Although scientific research has provided many different areas for high-performance anode materials, cathode electrodes with their lower capacities and higher costs have always been less researched. With the advancement of battery technology, the research community has recently been carrying out various studies both on the yield and the performance of the cathode materials for lithium-ion batteries.

One of the three-layer cathode electrode family is nickel, cobalt, and aluminum oxide (NCA) used in the positive electrode of electric cars and portable electronic equipment. The NCA cathode material provides higher capacities, energy and power efficiency, and is widely used in lithium-ion batteries. Besides these specifications, they are found

among the most promising positive electrode because of two reasons, lower synthesis costs and promising electrochemical properties.

The theoretical capacity of NCA cathode is 279.05 mAh /g. While these cathodes have the advantage of being produced via different synthesis methods, they can cause a decrease in capacity with time and degradation of the battery structure during cyclic tests due to micro and nanoscale cracks in the structures alongside reactions occurring over time.

To overcome the main problem of NCA cathode, as established earlier, I focused on the Nafion-coated NCA electrode. It is expected that Nafion coated NCA cathode material may improve ionic and electronic conductivity by covering the surface and prevent the side reactions and thus stabilize the capacity under cycles, which may lead to an increment in the life span of NCA cathode. NCA cathode active material was synthesized by a modified co-precipitation method at 750°C in an air atmosphere. The obtained NCA powder was characterized by X-ray diffraction, scanning electron microscopy and inductively coupled plasma-mass spectrometry. To understand the surface and structure of the electrode, the pristine and nafion-coated electrodes were also structurally characterized with X-ray diffraction, scanning electron microscopy, inductively coupled plasma mass spectrometry as well as battery tests that were carried out on both electrodes to understand their cell characteristics. The results were comparatively interpreted for nafion supported NCA cathode electrode and pristine NCA cathode.

**YÜKSEK ÇEVİRİM PERFORMANSLI LİTYUM İYON BATARYALARININ  
KATOT ELEKTROLARI İÇİN DİZAYN EDİLMİŞ NAFYON YÜZEY  
İYİLEŞTİRMELİ NCA KATOT MALZEMELERİ**

AYÇA YİĞİTALP

Material Science and Nano Engineering, M.Sc. Thesis, July 2019

Tez Danışmanı: Prof. Dr. Selmiye Alkan Gürsel

Doktoralı Öğretim Üyesi Alp Yürüm (Co-Supervisor)

**Anahtar Kelimeler:** Lithium-ion batarya, NCA katot, enerji uygulamaları, yüzey iyileştirmeli katot malzemeleri

**ÖZET**

Yüksek enerji yoğunlukları ve taşınabilir boyutları sayesinde, lityum-iyon piller günümüz teknolojisinde çok önemli bir rol oynamaktadır. Her ne kadar bilimsel araştırmalar yüksek performanslı anot materyallerine yönelik bir çok araştırma alanı sağlasalar da, anot elektrotuna göre daha düşük kapasiteye ve daha yüksek maliyetlere sahip olan katot elektrotlar, hep daha sınırlı araştırma alanında kalmıştır. Bu nedenle, katotların hem verimini hem de performanslarını arttırmak için son zamanlarda yoğun çalışmalar yapılmıştır.

Üç katmanlı katot elektrotlarından birisi; elektrikli arabalar ve taşınabilir elektronik ekipmanların katotlarında kullanılan nikel, kobalt ve alüminyum oksitli (NCA) katot malzemeleridir. NCA katot malzemesi, yüksek kapasiteleri, enerji ve güç verimliliğine sahip olmaları gibi özellikleri sayesinde lityum iyon bataryalarında yaygın olarak kullanılan elektrot malzemeleri içersinde yer alır. Bu özelliklerinin yanında, NCA katot malzemeleri diğer katotlara göre daha düşük maliyetlerle üretilebildikleri içinde gelecek vaadeden elektrotlar arasındadır. NCA katot malzemelerinin teorik kapasiteleri 279,05 mAh/g dır. Bu katotlar farklı sentez metotlarıyla üretilebilir olma avantajlarına sahip olsalarda, yapılarında bulunan mikro ve nano boyuttaki çatlaklar ve çevrim içi testler sırasında elektrolit yapısından da kaynaklı yan reaksiyonlar sebebiyle çevrimli testler sırasında kapasitenin düşmesine ve pil yapısının bozulmasına neden olmaktadır.

Başka bir deyişle, nafyon; iyonik iletkenliği ek bir direnç yaratmadan arttıran, yan reaksiyonları engelleyen ve katodun yapısında doğal veya kaplama sırasında varolan çatlakların arasını doldurarak katodu bir arada tutmayı sağlayan destek malzemesidir. Bu yüksek tezi çalışmasında, NCA katot malzemesinin sentezi 750 °C hava ortamında kimyasal çökeltme metodu kullanılarak yapılmıştır. Üretilen NCA toz malzemesi X-Işını Spektroskopisi (XRD), taramalı elektron mikroskobu (SEM), İndüktif Eşleşmiş Plazma-Kütle Spektroskopisi (ICP) ile incelendikten sonra elde edilen NCA katot elektrotlar, Nafion'un elektrokimyasal özelliklere ve NCA katot elektrotuna olan katkısını göstermek üzere; kıyaslamalı olarak rate kapasite testleri, cycling voltametre testleri ve elektrokimyasal empedans testleri ile incelenmiştir. Sonuçlar nafyon destekli NCA katot elektrodu ve saf NCA katodu şeklinde kıyaslanarak yorumlanmıştır.

*Işığıyla her daim yol gösteren melek annanem, canım dedem ve portakal kokulu  
çocukluğuma...*



## ACKNOWLEDGEMENTS

First and foremost, I would like to thank my supervisor, Prof. Dr. Selmiye Alkan Gürsel, and my co-advisor, Asst. Prof Dr. Alp Yürüm, and to my bachelor thesis advisor, Prof. Dr. Ali Arslan Kaya, for their huge support, motivation, patience and very kind attitude in every circumstance. Then, I would like to thank to our lead Ph.D. candidate, Adnan Taşdemir, and to all SU-ESC group members.

I would like to thank my lovely roommates, Özlem Can and Kankunlanach Kampuang, for their great support and for turning our stressful graduate life into fun and dramatic dances that I will miss. My thanks are also enlarged to my very old friend, Şükran Karademir, for always heartily supporting me and teaching me the way of seeing positive in every negative.

Finally, my deepest gratitude for my grandmother and grandfather for their patience, their great encouragement and for being there for me as always. I also thank to my family. Last but not the least, I am also grateful to my uncle, İbrahim Efdal Çiçekdemir, for being my inspiration in the academic path.

*Ayça Yiğitalp*

## TABLE OF CONTENTS

|  |             |
|--|-------------|
| <b>ABSTRACT.....</b>   | <b>IV</b>   |
| <b>ÖZET.....</b>   | <b>VI</b>   |
| <b>ACKNOWLEDGEMENTS .....</b>  | <b>IX</b>   |
| <b>LIST OF FIGURES.....</b>  | <b>XIII</b> |
| <b>LIST OF TABLES.....</b>   | <b>XV</b>   |
| <b>LIST OF EQUATIONS.....</b>  | <b>XVI</b>  |
| <b>ABBREVIATIONS AND SYMBOLS.....</b>  | <b>XVII</b> |
| <b>1. INTRODUCTION.....</b>  | <b>1</b>    |
| <b>1.1. Motivation of the Study .....</b>  | <b>1</b>    |
| <b>1.2. Historical Perspective of Batteries.....</b>   | <b>1</b>    |
| <b>1.3. Battery Overview .....</b>   | <b>2</b>    |
| <b>1.3.1. Working Principle of Lithium-Ion Battery .....</b>                                   | <b>2</b>    |
| <b>1.3.2. Thermodynamics of Batteries .....</b>  | <b>3</b>    |
| <b>1.3.3. Advantages of Lithium-Ion Battery .....</b>  | <b>4</b>    |
| <b>1.3.4. Limitations of Lithium-Ion Battery .....</b>   | <b>5</b>    |
| <b>1.4. Negative Electrode Materials of Lithium-Ion Batteries .....</b>                        | <b>5</b>    |
| <b>1.5. Layered Cathode Materials of Lithium-Ion Batteries.....</b>                            | <b>6</b>    |
| <b>1.5.1.Chronological Development and Limitations of Lithium-Ion Batteries’ Cathodes.....</b> | <b>9</b>    |
| <b>1.6. NCA Cathode Electrode for Lithium-Ion Batteries .....</b>                              | <b>11</b>   |
| <b>1.7. Modifications on NCA Cathode.....</b>  | <b>15</b>   |
| <b>1.7.1. The Role of Nafion on Batteries.....</b>   | <b>16</b>   |
| <b>1.8. Objectives.....</b>  | <b>16</b>   |

|           |   |           |
|-----------|---|-----------|
| <b>2.</b> | <b>EXPERIMENTAL</b>   | <b>18</b> |
| 2.1.      | Materials   | 18        |
| 2.2.      | Methods   | 18        |
| 2.2.1.    | Synthesis of NCA Powder                                     | 18        |
| 2.2.2.    | Preparation of Cathode Slurry                               | 18        |
| 2.2.3.    | Application of Nafion Surface on NCA Cathode                | 19        |
| 2.2.4.    | Assembling of Lithium-Ion Battery                           | 20        |
| 2.3.      | Characterization Methods                                    | 20        |
| 2.3.1.    | Material Characterization                                   | 20        |
| 2.3.1.1.  | X-ray Diffraction (XRD)                                     | 20        |
| 2.3.1.2.  | Scanning Electron Microcopy (SEM)                           | 22        |
| 2.3.1.3.  | Inductively Coupled Plasma Mass Spectroscopy (ICP-MS)       | 23        |
| 2.3.2.    | Electrochemical Characterization                            | 24        |
| 2.3.2.1.  | Cyclic Voltammetry (CV)                                     | 24        |
| 2.3.2.2.  | Electrochemical Impedance Spectroscopy (EIS)                | 25        |
| 2.3.2.3.  | Rate Capability   | 26        |
| 2.3.2.4.  | Charge Discharge Tests                                      | 26        |
| <b>3.</b> | <b>RESULTS AND DISCUSSION</b>                               | <b>27</b> |
| 3.1.      | NCA Powder Synthesis  | 27        |
| 3.1.1.    | XRD Tests   | 27        |
| 3.1.2.    | Scanning Electron Microscopy Tests                          | 29        |
| 3.1.3.    | Particle Size Distribution                                  | 31        |
| 3.1.4.    | Inductively Coupled Plasma Mass Spectroscopy (ICP-MS) Tests | 32        |
| 3.2.      | Electrochemical Characterization                            | 33        |
| 3.2.1.    | Cyclic Voltammetry (CV) Test                                | 33        |
| 3.2.2.    | Cyclability Tests   | 34        |
| 3.2.3.    | Electrochemical Impedance Analysis (EIS) Tests              | 38        |

|   |           |
|---|-----------|
| <b>3.2.4. Rate Capability Tests.....</b>  | <b>39</b> |
| <b>3.2.5. Overvoltage Tests .....</b>     | <b>40</b> |
| <b>4. CONCLUSION AND FUTURE WORK.....</b> | <b>42</b> |
| <b>5. APPENDIX.....</b>                   | <b>43</b> |
| <b>6. REFERENCES.....</b>                 | <b>45</b> |

## LIST OF FIGURES

|  |    |
|--|----|
| Figure 1-1. Components of Lithium-Ion Battery [9].   | 3  |
| Figure 1-2. Specific Energy vs. Energy Density of Various Anodes and Cathodes [1].   | 7  |
| Figure 1-3. Crystal Structure of LCO [21].   | 10 |
| Figure 1-4. Crystal Structure of LNO [23].   | 11 |
| Figure 1-5. Nickel Ions at the Lithium Sheets in Layered Structure of NCA Cathode [3, 30].   | 12 |
| Figure 1-6. Potential versus Specific Capacity of NCA Cathode Material [6,21].   | 13 |
| Figure 2-1. Illustration of Nafion Modified NCA Electrode.   | 19 |
| Figure 2-2. Lithium-Ion Coin Type Cell Assembly.   | 20 |
| Figure 2-3. The Diagram of the Working Principle of X-ray Diffraction and Bruker XRD D2 Phaser at Sabancı University (right) [49]. | 21 |
| Figure 2-4. The Working Principle of XRD (Bragg diffraction) [49].   | 21 |
| Figure 2-5. Schematic Representation of Origin and Types of Electrons (SE), (BSE) (AE) and X-rays [53].                            | 23 |
| Figure 2-6. Schematic Diagram of Inductively Coupled Plasma-Mass Spectrometer. .   | 24 |
| Figure 2-7. Voltammogram example [58] [59].  | 25 |
| Figure 2-8. Nernst Equation [57, 59].  | 25 |
| Figure 3-1. XRD Results of NCA Powder.   | 27 |
| Figure 3-2. 006/102 Double Peak of NCA.  | 28 |
| Figure 3-3. 110/018 Double Peaks of NCA.   | 28 |
| Figure 3-4. SEM Micrograph of NCA Powder.  | 30 |
| Figure 3-5. Nafion Coated NCA versus Pristine NCA in SEM.  | 31 |

|  |    |
|--|----|
| Figure 3-6. Histogram of NCA Powder.....   | 32 |
| Figure 3-7. Cyclic Voltammograms of Pristine NCA versus Nafion Coated NCA. ....                                | 33 |
| Figure 3-8. Capacity versus Voltage Test of both Electrodes at 0.1C.....                                       | 35 |
| Figure 5-1. (a) Specific Discharge Capacity versus Cycle Number; (b) Capacity versus Voltage of NCA cells..... | 43 |

## LIST OF TABLES

|   |    |
|---|----|
| Table 1-1. Carbon Based Negative Electrode Materials.....                           | 6  |
| Table 1-2. Cathode Electrode Materials Specifications of Lithium-Ion Batteries..... | 8  |
| Table 3.1. ICP-MS spectra.....  | 32 |

## LIST OF EQUATIONS

|              |       |    |
|--------------|-------|----|
| Equation 1-1 | ..... | 4  |
| Equation 1-2 | ..... | 4  |
| Equation 1-3 | ..... | 4  |
| Equation 1-4 | ..... | 4  |
| Equation 1-5 | ..... | 4  |
| Equation 1-6 | ..... | 4  |
| Equation 1-7 | ..... | 5  |
| Equation 2-1 | ..... | 24 |
| Equation 2-2 | ..... | 24 |



## ABBREVIATIONS AND SYMBOLS

|   |  |
|---|--|
| CE  | Counter electrode                            |
| C.V.  | Cell voltage                                 |
| CV  | Cyclic voltammetry                           |
| EIS   | Electrochemical impedance spectroscopy       |
| ICP-MS  | Inductively coupled plasma-mass spectrometry |
| LCO   | Lithium cobalt oxide cathodes                |
| LiCoO <sub>2</sub>  | Lithium cobalt oxide                         |
| LiFePO <sub>4</sub>   | Lithium iron phosphate                       |
| LiMn <sub>2</sub> O <sub>4</sub>  | Lithium manganese oxide                      |
| LiNiO <sub>2</sub>  | Lithium nickel oxide                         |
| NCA / LiNi <sub>0.80</sub> Co <sub>0.15</sub> Al <sub>0.05</sub> O <sub>2</sub> | Lithium nickel cobalt oxide                  |
| RE  | Reference electrode                          |
| SEI   | Solid electrode interface                    |
| SEM   | Scanning electron microscopy                 |
| SOC   | State of charge                              |
| WE  | Working electrode                            |
| XRD   | X-ray diffraction                            |

# 1. INTRODUCTION

## 1.1. Motivation of the Study

Although various cathode materials have been used to date, NCA cathodes have dominated the market and intensive research studies have been conducted since they have relatively high specific capacity, energy density and relatively lower cost and more importantly are non-toxic. While NCA cathode material is a key electrode type for lithium-ion batteries in various aspects that will be explained in further chapters, degradation of the NCA cathode material, micro sizes cracks and unwanted site reactions of this cathode occurring during cycling tests cause its life span to decrease and thus limit the application. Herein, our motivation is to eliminate the side reactions of NCA cathode and provide highly stable discharge characteristic under cycling tests at higher current rates. In line with the purpose, this research study is dedicated to the surface modified NCA synthesis by co-precipitation method, which brings forth superior electrochemical characteristics.

## 1.2. Historical Perspective of Batteries

Although the term battery was first used in 1749 by an American scientist, Benjamin Franklin, the first known batteries date back to 1738. In 1979, John Bannister Goodenough and his team found out that lithium metal oxides, also called ternary oxides, can be used as metal oxide in cathode terminal for lithium batteries [1, 2]. His team introduced the range of cell voltage by using lithium-cobalt oxide in the same year and this invention enabled lithium batteries to find a place in the market. Godshall et al. identified similar ternary oxides such as  $\text{LiMnO}_2$ ,  $\text{LiFeO}_2$ , and  $\text{LiFe}_5\text{O}_8$  in 1979.

After the discovery of storage of lithium in carbon-based material with a proper electrolyte, Sony corporation introduced carbon-based cell in the market and continued improvements performed on the same cell and then the term lithium-ion was used for batteries in performance of the carbon based cells [1, 3].

After ternary oxides had been frequently utilized in lithium-ion batteries, the science world shifted its focus on NCA cathode material,  $\text{LiNi}_{0.80}\text{Co}_{0.15}\text{Al}_{0.05}\text{O}_2$  with

specific discharge  $279.05 \text{ mAg}^{-1}$  for ten years [4]. The official reports have indicated that using NCA cathode active material has immensely grown in the industry since it provides promising results that will be mentioned in detail in upcoming sections, and hence batteries research and development has dramatically been growing day by day [1, 3, 5].

### **1.3. Battery Overview**

A battery is a combination of a single or multiple cells that converts chemical energy to an electrical energy by the virtue of oxidation and reduction reactions that primarily happens during the movement of electrons from one side to another through the electric circuit [3, 4]. Basic lithium-ion battery has two terminals, one of them is called cathode while the other one is the anode electrode [6].

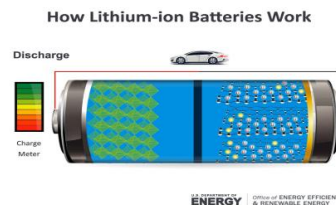
Day by day our energy sources are decreasing, therefore storage of energy and its conversion in an efficient way is one of the main research topics. In this perspective, batteries, fuel cells, and supercapacitors are significant inventions in today's world [3]. Lithium-ion batteries with their greater density, charge-discharge capacities, longer cycle life, being power reservoir and being used in portable devices are remarkably distinguished from their counterparts like fuel cells or supercapacitors. Moreover, lithium is the lightest and very electrochemically active (reactive) metal which provides higher energy and power density in batteries which is why it is frequently used in batteries in conjunction with different metals. Therefore, to widen and improve the application of batteries, physical combination of battery materials and their limitations can be overcome via modifications.

#### **1.3.1. Working Principle of Lithium-Ion Battery**

A battery consists of an electrochemical single or multiple cell that generate current by the virtue of electrochemical reactions and contain two terminals, an anode and a cathode. It differentiates from the other types of electrochemical power sources such as fuel cells, in terms of utilization of portable electronics which render them greatly in application area and is also linked to economic and environmental improvement.

In addition to the electrodes, an electrolyte is responsible for facilitating the positive lithium ions from one electrode to another. Other than the electrolyte, another component, separator, defined as a thin and nanoporous film, physically inhibits the connection between cathode and anode electrodes when conveying the ion transport by

the help of electrolytes through the terminals in the cell [7]. When a battery operates, the two terminals, anode and cathode, responsible for oxidation and reduction reactions, that take place in the electrodes depending on the affinity of the electrons of the electrodes according to potential differences at electrodes. During this phenomenon, one electrode, cathode, takes one electron and becomes negatively charged, while the other electrode, anode, loses that one electron and becomes positively charged [3, 8, 9]. To understand the logic of the electrode materials, it is essential to know the potential differences of the materials that are used as cathode or anode. Diagrammatically reactions and the components inside the lithium-ion battery for current generation are shown in Figure 1-1. The working principle of lithium-ion batteries can be further understood when the key cathode and anode reactions are known. This will be mentioned in the section 1.3.2. in detail.

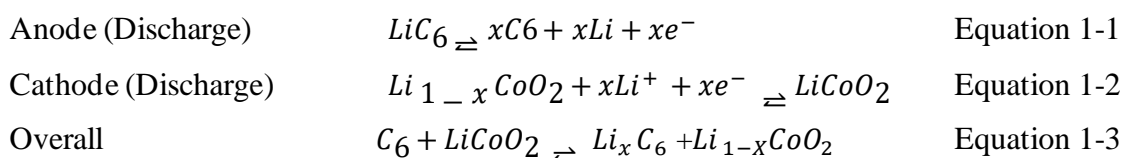


|  |   |   |
|--|---|---|
| <b>Cathode:</b> Stores lithium and release Li ions when battery is charging. | <b>Separator:</b> Allows lithium ion flow freely from the anode to cathode and vice versa. It also prohibits the flow of electrons. | <b>Anode:</b> Stores lithium and releases lithium ions when battery is discharging. |
|--|---|---|

Figure 1-1. Components of Lithium-Ion Battery [9].

### 1.3.2. Thermodynamics of Batteries

From the thermodynamic perspective, the main anode and cathode reactions that take place in the lithium-ion battery are indicated below and the overall equation for lithium for cobalt-based batteries are found in equations 1-1, 1-2 and 1-3 and 1-4. Also, the equation for lithium cobalt oxide/graphite type of the equations are shown in equations [10].



The change in the standard free energy  $\Delta G^\circ$  for this general equation 1-4 is represented as,

$$\Delta G^\circ = -nFE^\circ \quad \text{Equation 1-4}$$

Where, F is constant and  $E^\circ$  is standard electromotive force.

The reason for mentioning the  $\Delta G$  in the Equation 1-4 is equal to  $EV$ , which is also called cell potential. The changing of standard free energy of a cell reaction is one of the biggest motivations for the battery science since this changing allows the battery to work by conveying electric energy to external energy [10].

### **1.3.3. Advantages of Lithium-Ion Battery**

Lithium-ion batteries are differentiated from other types of batteries because of their portable nature, higher charge output and efficiencies as a main power source both for portable basic electronics and for electric cars and vehicles. They contain electrodes that are used in anode or cathode materials which provide them freedom in design and unique electrochemical characteristics.

For example, specific energy is the main advantage of lithium-ion battery technology. It is four times higher than lead-acid batteries [1, 3, 5]. Another plus is the specific power density. For example, in cathode of lithium-ion batteries specific energy density is between 252-695 Wh/L. Their specific power allows them to be used in multiple layer capacitors that are used in heavy application like electric equipment [13]. Also, higher power density of lithium-ion batteries is a determining advantage and very wanted criteria for improving the electric car technology. In addition to the advantages mentioned above, lithium-ion batteries can be made up of very small sizes. Cells of the batteries may be built to 1 mm in thickness, which has increased their utility in almost every portable electronics. Having diversity in size (very fine or big size batteries) is beneficial in different application areas.

In addition to the properties, secondary lithium batteries can be deeply cycled without losing their specific capacity for up to 500 cycles depending on the structure of lithium-ion battery as compared to the efficiency of cycling in lead-acid batteries which is 50%. The stored energy is used much more efficiently [12-14]. Depending on the structure of the batteries, some cells may be charged around 5 minutes. Discharging at

relatively high rates may provide an increment in the power of electric cars. Their self-discharge rates are much lower than that of other rechargeable batteries like nickel metal hydrates which enables them to preserve their initial charges for years. Lithium-ion secondary batteries have a smooth charge and discharge profile, which will be discussed in chapter 2 [14, 15].

Moreover, since synthesis methods and various techniques may be used for different types of a lithium-ion cells, several types of custom-tailored lithium-ion cells are also available.

#### **1.3.4. Limitations of Lithium-Ion Battery**

Although there are extensive synthesis methods and flexibilities in designing, yet expenses during production are still higher because of the “calendar life” and “capacity fade” [8, 10]. The crystal structure of the electrode materials undergo volume variation during lithiation/delithiation processes posing serious mechanical problems such as material cracking. Another limitation is their “deterioration” by extended cycles at high temperatures. Moreover, lithium-ion batteries are immensely prone to aging since they simultaneously charge and discharge in their lifetime. Lithium-ion batteries and battery technology with electrode materials are swiftly changing [11] Therefore, battery science is not mature science yet, however, this may also bring big advantages in the near future [8, 12].

#### **1.4. Negative Electrode Materials of Lithium-Ion Batteries**

Graphite and graphite based materials are common in anode electrodes. Graphite anode consists of mesh layers of carbon atoms. During charging, lithium ions are embedded on this mesh layers of carbon atoms which enable to increase the capacity up to  $372 \text{ Ah kg}^{-1}$ . For graphite cathodes, the production method of graphite is important as it determines the capacity, since the capacity decreases with an increase in crystallinity. Different types of graphite will offer differences in capacity which is generally between  $300\text{-}330 \text{ Ah kg}^{-1}$ . For example, spherical graphite provides the capacity range of  $300\text{-}330 \text{ Ah kg}^{-1}$ , while pristine (natural) graphite provides capacity of  $365 \text{ Ah kg}^{-1}$  [13].

Soft carbons, also called carbon black, are another type of source that are used in lithium-ion batteries. It is a certain fact that the main problem of cathodes in lithium-ion battery is their volumetric change between the charged and discharged states. These large

volume changes cause huge limitations on metal grains which are detrimental for cyclability. All these types of materials mentioned above are summarized along with their characteristics in Table 1-1. In addition, other type of electrode are Si and tin. The basic drawback in these anodes is the volume expansion which in turn form cracks. The crack formation causes the failure of the electrodes during charge and discharge tests.

Table 1-1. Carbon Based Negative Electrode Materials [14].

| <b>Materials</b>    | <b>Characteristics</b>  | <b>The role in Lithium-Ion Batteries</b>   |
|---------------------|---|--|
| <b>Graphite</b>     | Highly anisotropic properties in the basal plane and the edge sites; crystallite sizes 100nm and larger; surface area, interplanar [14] | Lithium intercalation rate depends on particle size, space and distribution, and morphology (spherical, flakes or fibers). True intercalation requires crystalline graphite: hexagonal |
| <b>Soft Carbons</b> | Graphitizable, unorganized carbon: petroleum coke and carbon black  | Heat treatment below graphitization provides a turbostratic form; low capacity owing to disorder between graphene layers.  |
| <b>Hard Carbons</b> | Nongraphitizable: glassy carbon and activated carbons   | Thermal stability of surface groups: carboxyl and lactone (evolve CO <sub>2</sub> at <math>500\text{ }^{\circ}\text{C}</math>); phenol and quinone (evolve CO at >600                  |

### 1.5. Layered Cathode Materials of Lithium-Ion Batteries

Cathodes of lithium-ion batteries have always been a restrictive component of batteries. Cathodes meet characteristic parameters in terms of specific capacity, cell potential and energy density of the batteries, their detailed analysis began in late 1990s [3]. Significant parameters like energy and powder density as well as cycle life, lean on the nature and the structure of cathode electrodes. The relations between specific energy

and energy density depend on different cathode materials as is shown in figure 1-2 [4, 15, 16].

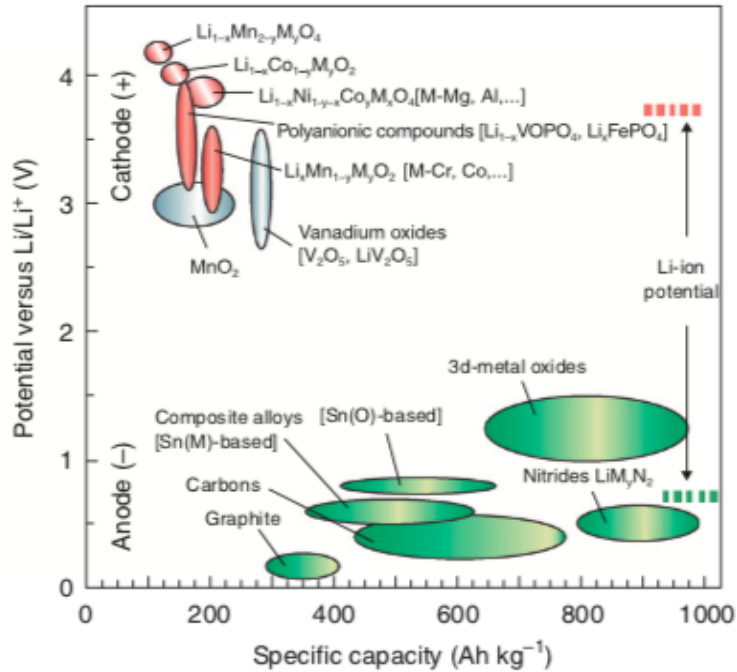


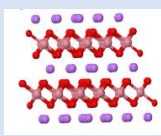

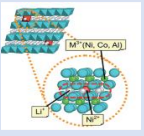


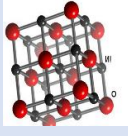
Figure 1-2. Specific Energy vs. Energy Density of Various Anodes and Cathodes [1].

Lithium ions when move through the positive electrode materials, the phenomenon is termed as intercalation. While the same lithium ions move out of the positive electrode materials, the phenomenon is termed as deintercalation. These stated phenomena are called discharge and charge, respectively.

In lithium-ion rechargeable batteries, a positive electrode should be lithiated before assembling the cell, unlike rechargeable batteries. Positive electrode materials can be lithium cobalt oxide, lithium nickel oxide, ternary oxides which are lithium nickel cobalt aluminum magnesium oxide, vanadium oxides or lithium iron phosphates. The cathodes are summarized in detail in Table 1-2 below [1, 12, 15, 17].



Table 1-2. Cathode Electrode Materials Specifications of Lithium-Ion Batteries [12, 18, 19].

| Property                    | LiCoO <sub>2</sub>   | LiFePO <sub>4</sub>   | Li <sub>0.80</sub> Ni <sub>0.150</sub> Co <sub>0.05</sub> AlO <sub>2</sub>   | LiMn <sub>2</sub> O <sub>4</sub>   | V <sub>2</sub> O <sub>5</sub>  | LiNiO <sub>2</sub>   |
|-----------------------------|--|---|--|--|--|--|
| Cell Voltage                | 3.7 V  | 3.5 V   | 3.0-4.2 V  | 3.6 V  | 3.0 V  | 3.6 V  |
| Cycle Life                  | >1000  | >1000   | >500   | >300   | >1000  | >500   |
| Theoretic Specific Capacity | 137 Ahkg <sup>-1</sup>   | 170 Ahkg <sup>-1</sup>  | 273 mAhg <sup>-1</sup>   | 272 mAhg <sup>-1</sup>   | 442 Ahkg <sup>-1</sup>   | 192 Ahkg <sup>-1</sup>   |
| Specific Energy             | 90-140 Whkg <sup>-1</sup>  | 100 Whkg <sup>-1</sup>  | 120 Whkg <sup>-1</sup>   | 160 Whkg <sup>-1</sup>   | >450 Whkg <sup>-1</sup>  | 442 Whkg <sup>-1</sup>   |
| Crystal Structure           |       |  |   |                          |                         |                   |
| Characteristic              | Used in the market, higher energy density, hazardous for environment because of cobalt | Termed as olivine, suitable for doping and modification of surface                | High charge provides thermal runaway, electrical, automobile application such as Tesla, suitable for surface modifications | Also termed as spinel, like olivine suitable for plug-in practices. spinel has lower capacity than olivine | Studies about surface oxygen vacancies show that the oxygen species is bound quite strongly to the surface | Due to its low content of lithium structure at elevated temperature capacity fade is frequently seen |

In addition to Table 1-2, lithium cobalt oxide (LCO) cathodes consist of 60% cobalt which is equivalent to 50% of the total weight of the cathode. Even though, this kind of cathode is frequently used in the market, and because of cobalt content it is associated as a hazard for the environment which is linked to its low safety performance.

Another cathode is LiFePO<sub>4</sub>, termed as olivine. One of the characteristics of this cathode is having stable phase at elevated temperatures. Phase change helps to provide a smooth voltage versus charge characteristics. The voltage range of 3.4 to 3.5V is well fitted for polymer-based solid electrolyte. “The existence of 1D channels for Li<sup>+</sup>-ion motion [in that type of cathode] imposes two constraints: (1) the Li channels must not be blocked by either disorder of the Li and Fe atoms or by the presence of a foreign phase; (2) the cathode particle must be small without stacking faults that block the channels” [12].

*Li<sub>x</sub>Mn<sub>2</sub>O<sub>4</sub> spinel cathodes* have crystallographic transformation from cubic to tetragonal phases. Their cycling ability is very low because of Jahn Teller distortion, which is defined as a geometric distortion of systems which are not uniform. Also, its reversible capacity is 72 mAh/g and energy density is 853 Wh/kg achieved at a low charge-discharge rate which is around 3.33 mA/g [2, 12, 20].

*Metal oxides like V<sub>2</sub>O<sub>5</sub> and LiNiO<sub>2</sub>* are layered oxide cathodes for lithium-ion batteries. Oxides provide more stable oxidation state of transition metal atoms. In addition, only when the structure is comprised of vanadyl or molybdyl, the layer of oxides is stable in V<sub>2</sub>O<sub>5</sub> or MoO<sub>3</sub> and LiNiO<sub>2</sub> will be discussed in section 1.5.1.

### **1.5.1. Chronological Development and Limitations of Lithium-Ion Batteries'**

#### **Cathodes**

*Lithium cobalt oxide (LCO)* is the first candidate for battery technology. However, the structural stability of these cathodes is concerned with the reactions that are also termed as “parasitic reactions” which occur at the boundary of a cathode and the electrolyte grounds the cell’s lifetime. The speed of these reactions heavily depends on the surface’s catalytic behavior. To eliminate the probability of having these outcomes, modifying the structure of the cathode by another element, nickel, the electrolyte modifications in LiCoO<sub>2</sub> cathode as core-shell may be an alternate solution. Also, stopping the migration of lithium-ion towards the layers of LCO that are shown in Figure1-3. is not plausible which declines the electrochemical activity in LCO. Figure1-4 shows the crystal structure of LCO. For Li<sub>1-x</sub>CoO<sub>2</sub> cathode, the reversible phase transition from trigonal into the monoclinic structure only occurs when x is 0.5, but the value of x is not always 0.5.

Higher values of x cause an unstable structure of Li<sub>1-x</sub>CoO<sub>2</sub> in organic electrolytes such as LiPF<sub>4</sub>. The unstable structure then ends up with cobalt loss, which lead to capacity fade. Cobalt moves from the structure in the lithium layer and results in huge capacity lost [21]. Therefore, at the range of  $0 \leq x \leq 0.5$ , LCO’s theoretical capacity is 272 mAh/g. In the same range, it also gives a plateau.

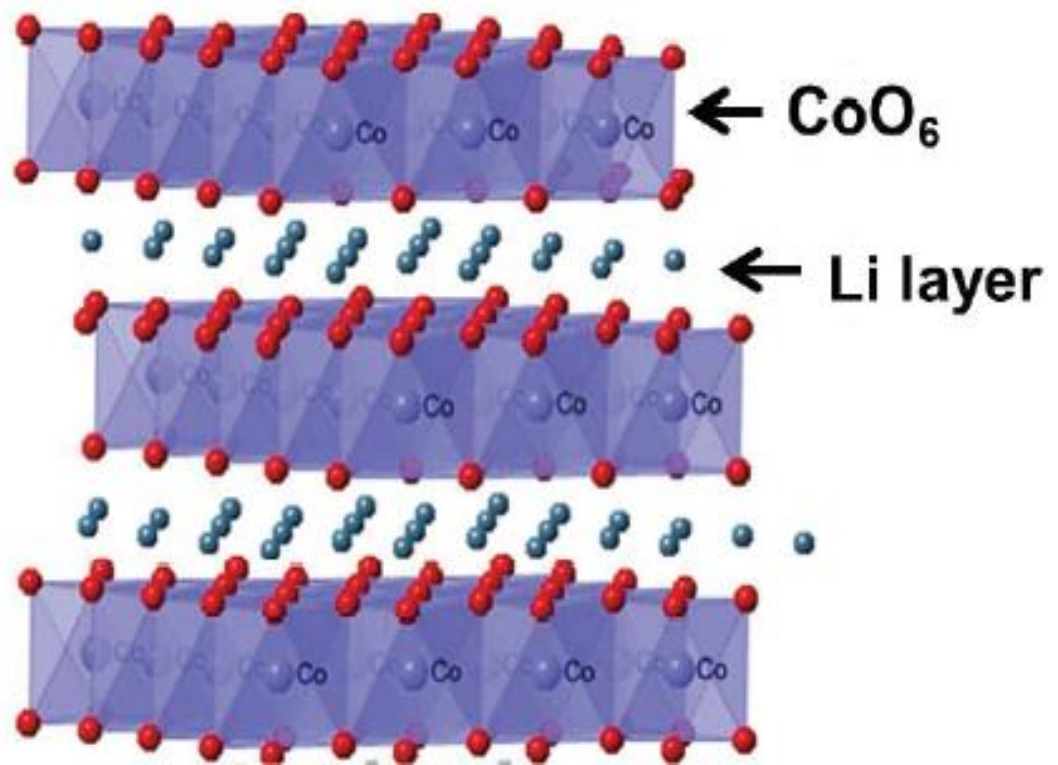


Figure 1-3. Crystal Structure of LCO [21].

*Lithium nickel oxide (LNO)*, also known as nickel rich cathodes, are the type of cathodes frequently used in lithium-ion batteries due to their moderate reversible capacity and lower cost. However, the surface of the electrode, which is not electrochemically stable, causes to degrade and ends up with LiOH and Li<sub>2</sub>CO<sub>3</sub> which heavily remove the lithium ions from the host structure. Typical LNO structure is seen in Figure1-3. During charge and discharge tests the residual compounds which were mentioned in the previous sentence repeatedly building in the structure, which in turn tremendously creates an extra barrier for charge transfer. Moreover, Ni<sup>+2</sup> ions could prevent the diffusion of lithium and in turn courses a capacity fade. In order to overcome these stated issues, adding a slight amount of nickel atoms linked with cobalt and aluminum atoms to modify the structure which lead to another cathode electrode in lithium-ion batteries: NCA and NMC cathode [22].

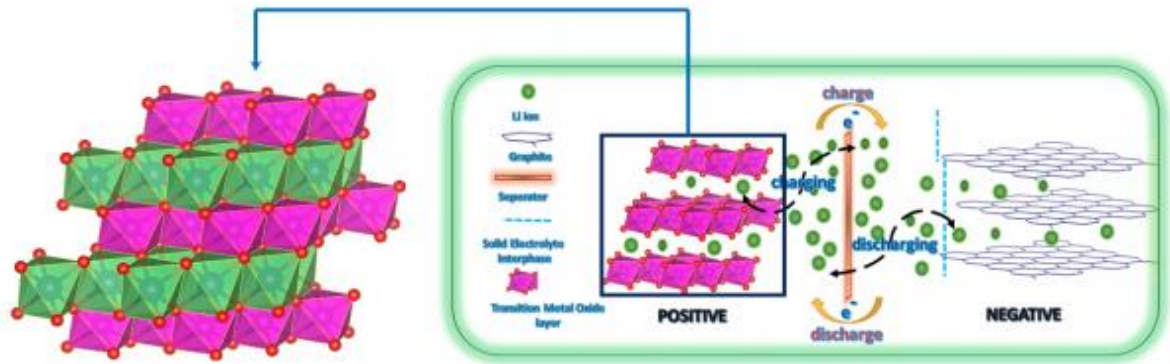


Figure 1-4. Crystal Structure of LNO [23].

*Nickel manganese cobalt oxide (NMC)* is another type of cathode. Specific discharge capacity varies depending on the quantity of constituents that are nickel, manganese and cobalt. This type of cathode, like NCA cathodes, provides higher capacity and lower weight, which means that they provide much dense energy which is stored and thus provides better extended battery life. These cathodes have been used in several car brands such as Panasonic, Tesla, and BMW i3. While NMC have around 80% Ni and 15% Co doped, both NMC and NCA when compared in terms of their electrochemical properties, are slightly different from each other. For example, the operating voltage range in NMC cathode is between 2.8-4.6 V, while this range for NCA is between 3.0-4.3 V.

### 1.6. NCA Cathode Electrode for Lithium-Ion Batteries

Until this section, it is seen that different criteria and cathode/anode materials may be used to build up commercial lithium-ion batteries. In the midst of the cathode materials, many of the lithium-ion batteries utilize Ni and Co-rich cathodes since they have relatively higher discharge capacity and excellent electrochemical cycling [24, 25]. Among these cathodes, ternary oxide cathode materials have been extensively researched and scrutinized in today's battery technology.

One of the ternary oxide group members is nickel cobalt aluminum oxide cathode material ( $\text{LiNi}_{0.80}\text{Co}_{0.15}\text{Al}_{0.05}\text{O}_2$  /NCA). This cathode which is highly used in today's technology especially in electric vehicles due to its thermally stability which in turn, reduces the safety considerations. Also, both nickel and lithium-rich cathodes like NCA are dominant in industrial applications. More specifically, around 48% of the theoretical

capacity of NCA (276.5 mAh/g) is effectively observed in voltage tests with the range of 3.0-4.2 V, which back as high discharge capacity [24-27]. In the presence of cobalt and aluminum, the structure stabilizes the layered structure and provides excellent stability and electrochemical reactivity with a specific capacity as mentioned above [28]. Another benefit of NCA cathode is that it allows ion doping that provides the electrochemical improvement on electronic and ionic conductivities. While at the same time, reducing the cation mixing. Cation mixing is defined as cation disorder of having a similar ionic radii of elements that stabilizes the crystal structure that is seen in Figure 1-3 [29].

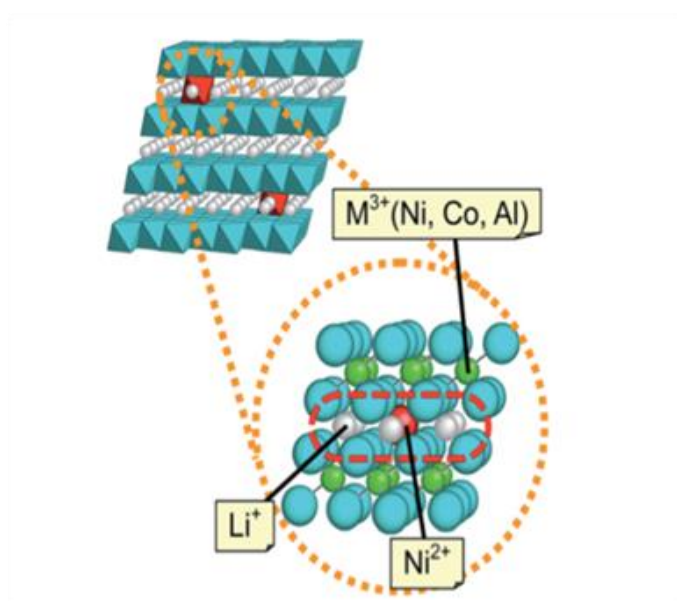


Figure 1-5. Nickel Ions at the Lithium Sheets in Layered Structure of NCA Cathode [3, 30].

In addition, electrochemical results have shown that intercalation material exhibits solid solution behavior during the extraction of lithium, which in turn provides relatively flat surface characteristic of charge/discharge. The energy density of NCA is 640 Wh/kg and its power density is 220 Wh/kg. These values can be slightly vary depending on the synthesis, slurry and assembling characteristics. Capacity versus potential graph of NCA cathode is comparatively shown in Figure 1-6 [5, 31]. NCA cathode when compared to other cathode material provide the highest specific capacity as well as high potential which makes NCA cathode a powerful candidate for several electronic applications.

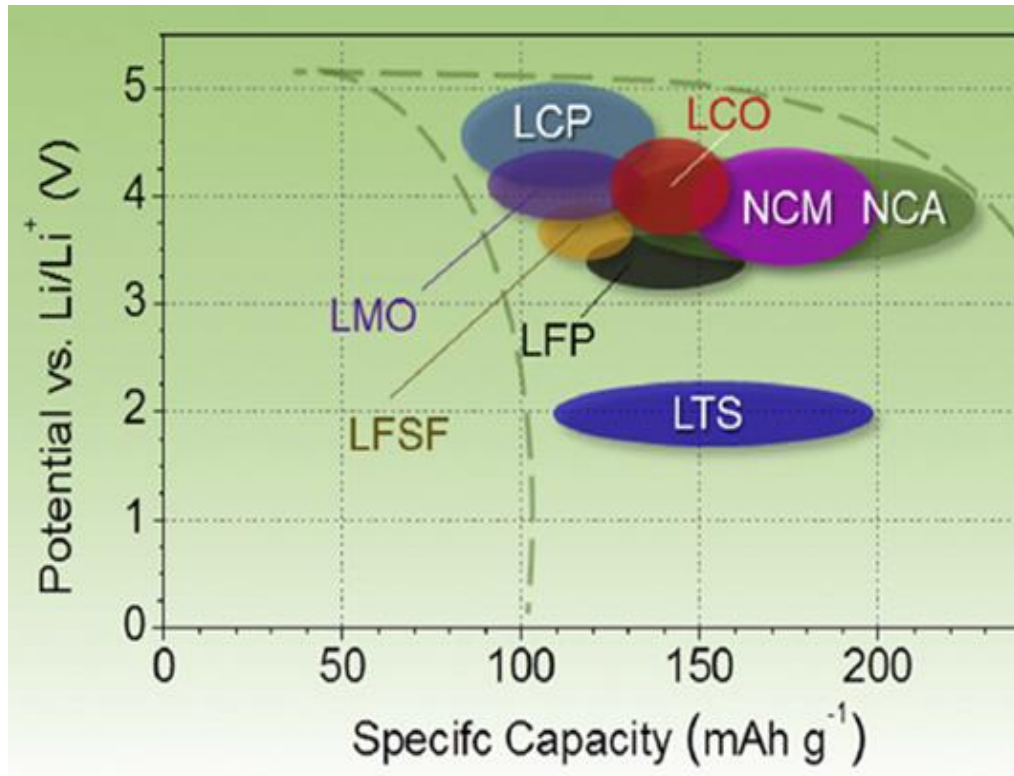


Figure 1-6. Potential versus Specific Capacity of NCA Cathode Material [6,21].

There are different techniques that can be used to synthesize NCA cathode powders. The first method is *solid state synthesis*. In this technique, an elevated sintering temperature and very high oxidative atmosphere is needed, but this in turn may bring environmental issues [6]. The obtained NCA via solid state synthesis provide a better electrochemical characteristic as compared to the other material oxides. Therefore, this limitation hinders commercialization. On the other hand, this problem could be minimized by applying a two-step solid state method. First step involves; heat treatment of highly crystalline sintered material at lower temperature. In the second step, relatively higher temperature sintering assists the formation of NCA.

The solid-state process can also be applied in an oxygen atmosphere. In this method, solid reactants which are,  $\text{LiOH}$ ,  $\text{Ni}_2\text{O}_3$ ,  $\text{Co}_2\text{O}_3$ ,  $\text{Al}(\text{OH})_3$ , are used for obtaining NCA cathode. The starting materials are mixed to have a smooth and homogenous structure. After the pre-heating step, they are placed under a flow of oxygen at high temperature for more than a day. This technique provides higher capacity retention even after 20 cycles [31-33].

The solution-based method is *ternary oxide precursor method*. In this method, oxalic acid is directly mixed with metal salts. Then raw material can be sintered at 450°C for 6 hours without filtering. After sintering, the precursor is mixed with LiOH and sintered at 550°C for 8 hours and at 750°C for 24 hours, respectively. This method provides highly crystalline particles. However, polyhedral NCA in this method may not be homogenous in structure. The initial discharge capacity is around 196 mAhg<sup>-1</sup> and the capacity retention is 76.1% after 100 cycles [31, 34, 35].

Another synthesis method is the *conventional solution route* synthesis which enables better mixing than the conventional solid-state methods. It requires a dissolved material in the water at room temperature. The NCA is obtained from metal acetates. The homogeneity of the solution is a key consideration in this technique and it is a simple and low-cost method [31, 32].

*Co-precipitation* is one of the promising methods to obtain cathode material within nano-range. In this method, NaOH as a hydroxide source and Na<sub>2</sub>CO<sub>3</sub> as the carbonate source are utilized for synthesis. Guilnard *et al.* have worked on this synthesis method to produce NCA cathode synthesized by a single-step co-precipitation method as a cathode material for Li-ion batteries. LiOH is used as the lithium source in single step co-precipitation method and the product NCA(OH)<sub>2</sub> is obtained. The obtained particle structure is highly crystallized with, highly isotropic and homogenous in shape. The size of the particle was 0.5 μm. In addition, the discharge capacity was 150 mAh.g<sup>-1</sup>, and this value remained at 130 mAh.g<sup>-1</sup> even after 50 cycles (0.05 C). These discharge values resulting from this technique are much lower than other methods mentioned above which have lower electrochemical properties [24, 35-37].

Synthesis techniques for NCA cathodes have grabbed great interest of battery scientists in the past decades. It provides variety in synthesis methods, requires relatively higher discharge capacity within cathode and obviously great power and energy density. Even though they are vastly researched, the biggest disadvantage of LiNi<sub>0.80</sub>Co<sub>0.15</sub>Al<sub>0.05</sub>O<sub>2</sub> (NCA) cathode are its side reactions occurring during cycling tests and limit the cycling performance, which in turn decrease the life span of the electrode.

On the other hand, LiPF<sub>6</sub>-based electrolyte decomposes into hydrogen fluoride (HF) during hydrolysis. HF can erode the transition-metal elements on cathode and cause an irreversible damaged to the crystal structure of NCA cathode. As a result of this phenomena the capacity fade, which end up with failure is seen in NCA [38].

Moreover, NCA has micro and nano size cracks that ultimately affect the discharge capacities and its cycle ability during tests. The crystal structure of NCA is hexagonal which is shown in Figure 1-5. Microcracks are because of heavily extended NCA structure under voltages. Transformation of phases from H2 to M causes the extension and this extension becomes severe and causes microcrack formation. Also, the electrolyte that is traditionally used in lithium-ion battery is  $LiPF_6$  decomposes after around 4.2V which is very near to cut-off voltage range [4, 33, 39, 40]. This decomposition continuously lasts and results in decreased discharge capacity as well as coulombic efficiency [17, 41, 42].

### 1.7. Modifications on NCA Cathode

As stated earlier, limitations and drawbacks have led the science world into modifications on NCA cathode materials. In order to eliminate the side reactions arising from the electrolyte and electrode, scientists have tried many different surface modifications to positive electrodes. These modifications have been reported in diverse studies in the literature. For instance,  $\alpha$ - $MoO_3$  particles are used on  $Li_{0.20}Mn_{0.54}Ni_{0.13}Co_{0.13}O_2$  cathode and it is reported that a thin layer of  $\alpha$ - $MoO_3$  particles changes the electrochemical performances during charge and discharge tests [34].

Another example is carbon coating on  $LiNi_{0.8}Co_{0.15}Al_{0.05}O_2$  cathode as the layer provides a much high diffusivity in the structure of a Li-ion battery and decreases the mechanical stress, which in turn provides huge recovery on the discharge profile [4, 31, 43].

The third modification is the effect of gradient boracic polyanion-doping on NCA cathode materials. Chang *et al.* have shown that the boracic polyanion-doping of NCA cathode has declined the capacity fade by  $7.4 \text{ mAhg}^{-1}$ , which corresponds to a significant change in the electrochemical properties [29].

Encapsulating NCA cathode is another type of surface modification that permitted on NCA cathodes. Jiang *et al.* have researched on nickel-rich layered structures of transition metals. In this research, the Ni-rich cathode was prepared by mechanically mixing the constituents and wrapping it with graphene [34].

Similarly, wrapping the Ni-rich cathode with lithium lanthanum titanium oxide inorganic film; shortly termed as LLTO is another type of surface modification which Kim *et al.* claim that it prevents the side reactions of nickel-rich cathodes, thus treats on capacity [44, 45]. All these surface modifications on nickel-rich cathodes are rather



complex to implement and require more energy than Nafion surface modification on NCA cathode.

### **1.7.1. The Role of Nafion on Batteries**

The expansion of Nafion is sulfonated tetrafluoroethylene based fluoropolymer-copolymer. It is also termed as perfluorosulfonated membranes. Nafion is frequently used in energy applications, that are primarily in proton exchange membrane fuel cells as a proton conductor due to its very high thermal, mechanical and chemical stability as well as superior proton conductivity. Besides being used in fuel cells, Nafion is utilized in NiMH batteries as it provides better electrochemical characteristics on the electrode-Nafion interface of NiMH battery (Nafion coated Mg50Ni50 anode) [46]. In this research, the reason for using Nafion on NCA cathode is its being superior ionic conductivity, high chemical stability as well as being a protective lamination on NCA cathode.

### **1.8. Objectives**

The studies on NCA cathodes have indicated promising results for battery applications as it is seen in the previous section. Its superior discharge characteristics, variety of synthesis methods and its tolerance towards battery technology were reported in various articles as mentioned in the literature review above.

Additionally, NCA with its surface modification improvements provide superior electrochemical properties and provides wide research areas and may create a significant improvement for commercialized NCA cathode material. In accordance to the literature, the most promising technique is the surface and structural modification of NCA cathode necessary to achieve superior properties. Considering pre-investigation, this thesis attempts to give a perception in the area of modified NCA cathode for investigating its electrochemical properties. In accordance with this purpose, our motivation is to eliminate the side reactions of NCA cathode and provide highly stable discharge characteristic under cycling tests. In line with this goal, NCA cathode was developed by a modified co-precipitation method that provides more fine and dispersed powders. Surface modification was then applied with Nafion coating on the synthesized NCA cathode powders. To the best of our knowledge, such surface modification has not been reported on NCA cathode electrode. Nafion is thought to help create a stable discharge profile under multiple cycles and prevent the side reactions by creating a protective cover

between electrode and electrolyte, which in turn prevent the capacity fade under cycling tests. After electronic and structural properties of the powders are confirmed and explained, all the electrochemical tests were performed, the results are comparatively shown and discussed both for pristine NCA and Nafion coated NCA.

In future research, further modifications on NCA cathode can be built upon this study. An additional surface modification to Nafion modified NCA cathode may be continuously developed based on this research. All these surface or structure modifications on NCA cathode materials will shed light on the battery technology.

## 2. EXPERIMENTAL

### 2.1. Materials

In order to synthesize  $\text{LiNi}_{0.80}\text{Co}_{0.15}\text{Al}_{0.05}\text{O}_2$  (NCA) powder, following materials were used:  $\text{Co}(\text{CH}_3\text{CO}_2)_2 \cdot 4 \text{H}_2\text{O}$  (cobalt II acetate tetrahydrate, 98%),  $\text{Ni}(\text{CH}_3\text{CO}_2)_2 \cdot 4 \text{H}_2\text{O}$  (nickel II acetate tetrahydrate, 98%),  $\text{AlCl}_3$  (aluminum chloride, 98%, also known as aluminum trichloride) and  $\text{C}_2\text{H}_2\text{O}_4$  (oxalic acid, 98%) were used as starting materials.  $\text{NH}_3$  (Ammonia) and 200 mL of distilled water were used. After sintering, the stoichiometric amount of  $\text{C}_2\text{H}_3\text{LiO}_2$  (lithium acetate) was used to obtain a final composition. All the chemicals were supplied by Sigma-Aldrich and they were used without further purification. For preparing the cathodes, Carbon Black<sup>®</sup> and PVDF<sup>®</sup> (polyvinylidene difluoride) were used to obtain appropriate battery slurry. In assembling the battery, Li anode chips,  $\text{LiPF}_6$  solution in ethylene carbonate (EC)/diethyl carbonate (DEC) (1:1 vol/vol, Sigma Aldrich), CR2032 type coin cells and Polypropylene separator (Celgard) were used. Nafion is Fuel Cell Earth. 15 % wt is used for surface modification.

### 2.2. Methods

#### 2.2.1. Synthesis of NCA Powder

As mentioned earlier, the starting materials used were  $\text{Co}(\text{CH}_3\text{CO}_2)_2 \cdot 4 \text{H}_2\text{O}$ ,  $\text{Ni}(\text{CH}_3\text{CO}_2)_2 \cdot 4 \text{H}_2\text{O}$ ,  $\text{AlCl}_3$ , and  $\text{C}_2\text{H}_2\text{O}_4$ . After they were completely dissolved in 200 mL of distilled water with a molar ratio of  $\text{Ni}_2+\text{Co}_2+\text{Al}_3+ = 80:15:5$ , 10 mL of  $\text{NH}_3$  was added to the solution for precipitation. The solution was then continuously stirred for around 2 hours. The obtained mixed solution was placed in an oil bath at  $80^\circ\text{C}/10$  hours until the precipitates formed. The obtained  $\text{NiCoAlC}_2\text{O}_4$  powder was then sintered at  $500^\circ\text{C}$  for 8 hours in an air atmosphere. Sintered powder was completely mixed with a stoichiometric amount of  $\text{C}_2\text{H}_3\text{LiO}_2$  and mortared. After mortaring, final calcination was then applied at  $750^\circ\text{C}/24$  hours in an air atmosphere.

#### 2.2.2. Preparation of Cathode Slurry

After obtaining the powder, 5 mL of NMP (N-methyl-2pyrrolidone, Sigma Aldrich) was poured to obtain a uniform and viscous slurry. The viscous slurry was stirred overnight. The slurry was coated on to carbon paper and then dried at  $120^\circ\text{C}$  overnight in a vacuum oven. Heat treatment was performed on the dried electrode (hot

pressed at 120°C/2 minutes) equally both for the top and bottom plates. Until here, the procedure was the same for Nafion coated electrodes. After drying and heat-treatment, electrodes were obtained, half of these electrodes were coated with Nafion® (Nafion was diluted to 50%). After coating them with Nafion, they were dried at 70°C in an oven. To assemble the cells and show the electrochemical differences between the electrodes, CR2032 type coin cell was used in a glove box using Li chipped anode. Electrochemical measurements were carried out for coin type cells that consisted of both pristine NCA and Nafion coated NCA.

### 2.2.3. Application of Nafion Surface on NCA Cathode

After NCA cathode electrode is obtained, Nafion is utilized for surface modification on ready NCA cathode. Before implementation of the Nafion solution, %30 diluted. The brand of Nafion is Fuel Cell Earth (15% wt) the solution should homogeneously be mixed and should be fully in a liquid form without having foam. Dripping method is then applied with a 100-microliter pipette from a 20 cm distance to the surface of the NCA electrode without creating any contact. The last step is drying. Nafion modified NCA electrode should be dried overnight at 40 °C- 45°C in an open atmosphere. CR2032 coin cells were assembled for battery and electrochemical tests. Figure 2-1 indicates the surface modification of Nafion on NCA electrode.

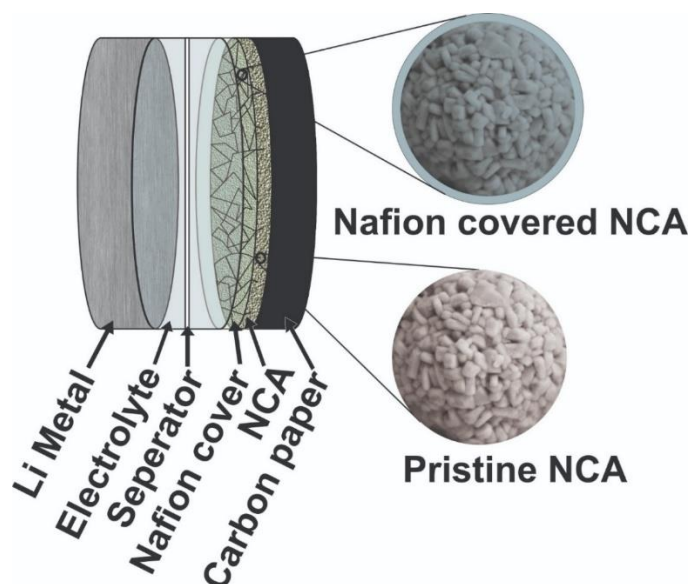


Figure 2-1. Illustration of Nafion Modified NCA Electrode.

## 2.2.4. Assembling of Lithium-Ion Battery

After preparing the cathode slurry, NCA cathodes were placed in coin type cells. Figure 2-2 below indicates the elements. After placing the components, manual pressing was applied in order to obtain sealed coin cell.

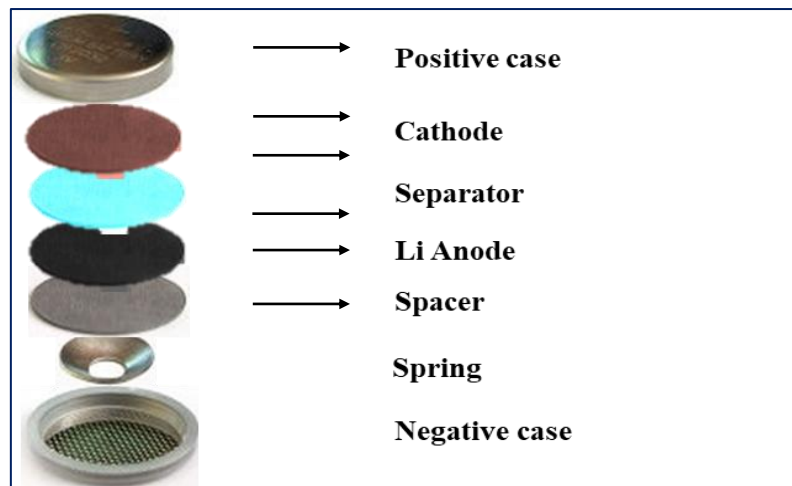


Figure 2-2. Lithium-Ion Coin Type Cell Assembly.

## 2.3. Characterization Methods

### 2.3.1. Material Characterization

#### 2.3.1.1. X-ray Diffraction (XRD)

X-ray diffraction is one of the physical material characterization technique. This method gives information about the material crystallinities. As is evident from its name, this technique uses x-rays that diffracts the beam into the detector. Both the beam and detector are rotated through an angle, that provides positioning of the generated beam in coordination with the position of the specimen [47]. Each material has a specific diffraction pattern that is related to the specific intensity of beam which is diffracted as seen in Figure 2-3 [48].

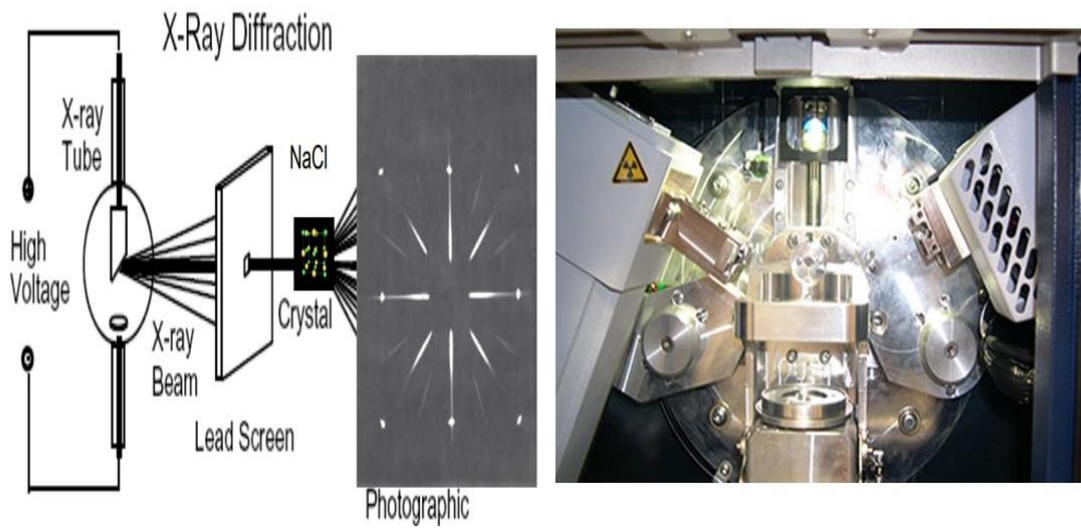


Figure 2-3. The Diagram of the Working Principle of X-ray Diffraction and Bruker XRD D2 Phaser at Sabancı University (right) [49].

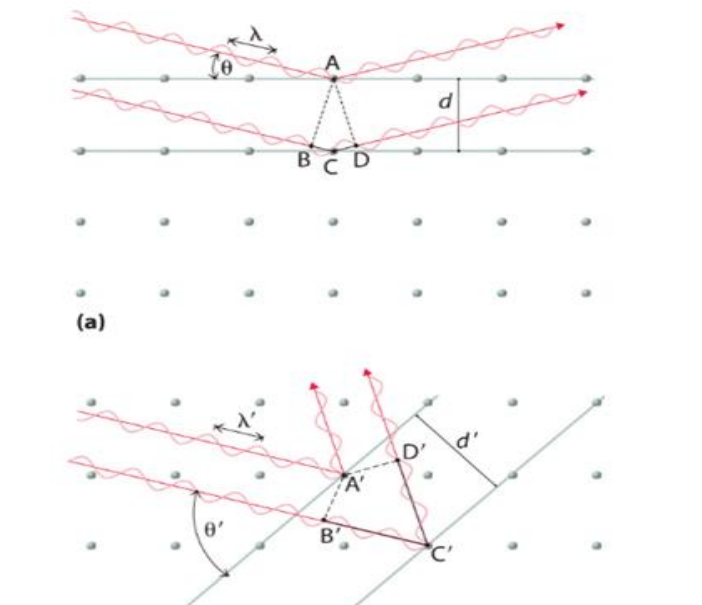


Figure 2-4. The Working Principle of XRD (Bragg diffraction) [49].

Bragg equation indicates the relationship between the angular distribution of the peak intensities from the lattices. The distance that is taken between the incident and

diffracted beam is calculated by the formula stated below. According to the Equation 2-1,  $n$  is an integer determined,  $\lambda$  is the wavelength of x-rays of moving electrons, protons and neutrons,  $d$  is the spacing between the planes in the atomic lattice, and  $\theta$  is the angle between the incident ray and the scattering planes [47, 48, 50]. Different plains having a different  $d$  spacing will have different diffraction angles and therefore will give different patterns that is schematically seen in Figure 2-4.

$$n\lambda = 2d\sin\theta \quad \text{Equation 2-1}$$

In addition to the Bragg's equation, the crystallinity size is calculated by using Scherer Equation 2-2 given below. Where,  $D$  is average dimension of the crystallites,  $K$  is the Scherer constant,  $\lambda$  is the wavelength of the X-rays and  $\beta$  is the integral breadth of the reflection.

$$D = K\lambda/\beta\alpha \quad \text{Equation 2-2}$$

#### 2.3.1.2. Scanning Electron Microcopy (SEM)

Scanning electron microscopy (SEM) is another type of powder characterization technique. It provides topographical images from surface analysis of conductive samples. SEM also gathers information about chemical composition. In an SEM, electrons are generated by applying current to an electron gun. The current through the electron gun heats up and electrons are emitted.

When the generated beam interacts with the sample, several beams and different types of electrons are produced. The beams or electrons could either be x-ray with higher energies or backscattered electrons with lower energies. Figure 2-5 schematically represents the key interaction processes and information volumes.

When the electrons interact with sample's atoms, they produce different signals which provide sources of surface topography and composition of the sample which is seen on the right side of Figure 2-5. The working principle of SEM is illustrated below [51, 52].

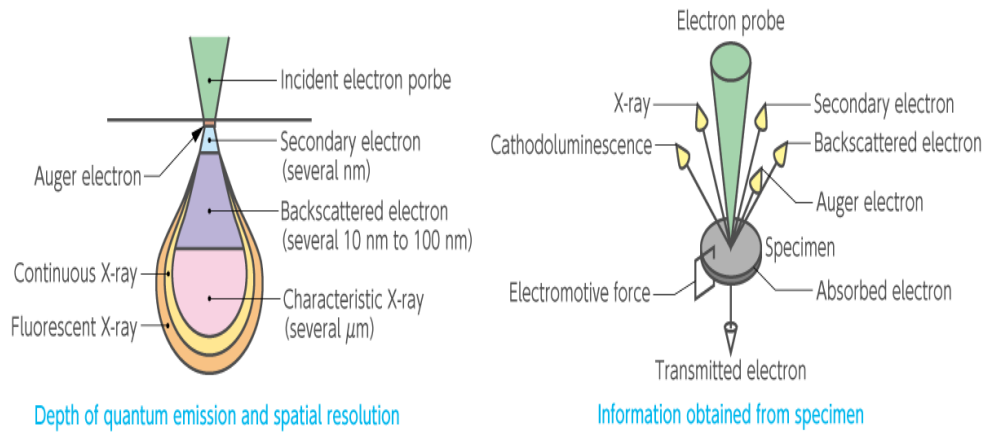


Figure 2-5. Schematic Representation of Origin and Types of Electrons (SE), (BSE) (AE) and X-rays [53].

### 2.3.1.3. Inductively Coupled Plasma Mass Spectroscopy (ICP-MS)

One of the mass spectroscopy measurement is inductively coupled plasma mass spectroscopy (ICP-MS). This spectroscopy measures both the concentrations of metal and non-metals [54]. The technique can determine the periodic table elements from microgram to nanogram levels. The ICP-mass spectrometer is also used in different industries other than metallurgy and materials science. This technique utilizes an ionization source, which decomposes sample phases into its constituent elements and transforms the elements into gases. It uses argon gas and the energy is coupled to an induction coil for generating the plasma. Figure 2-6. shows the working principle.



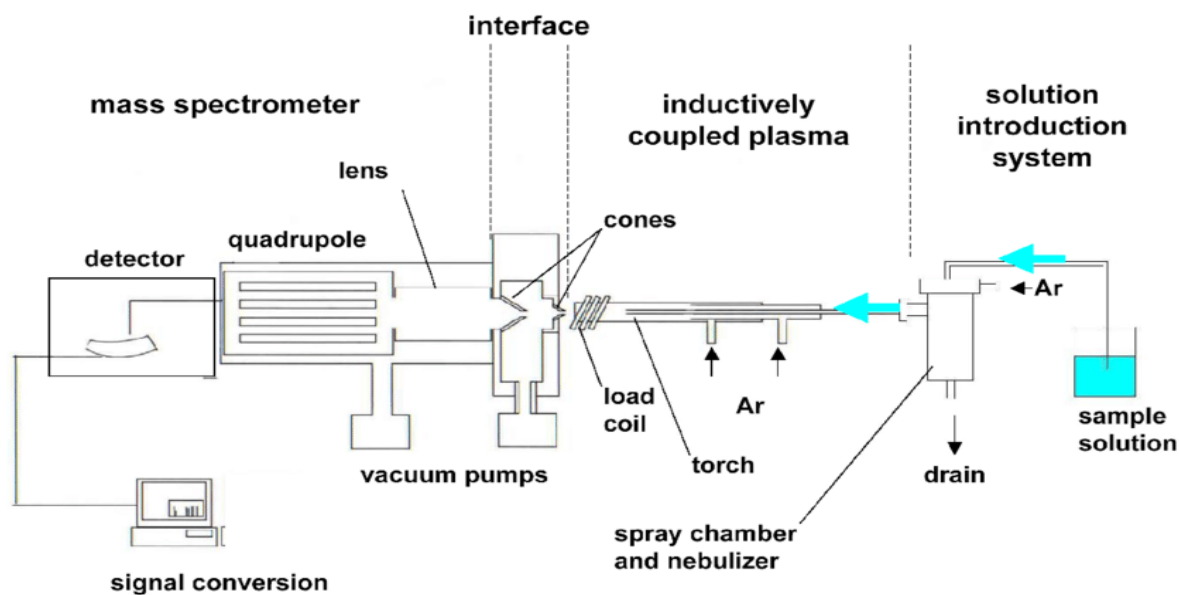


Figure 2-6. Schematic Diagram of Inductively Coupled Plasma-Mass Spectrometer.

## 2.3.2. Electrochemical Characterization

### 2.3.2.1. Cyclic Voltammetry (CV)

Cyclic voltammetry (CV) is one of the electrochemical techniques, which determines the current under known conditions at specific potentials [55, 56]. In other words, it utilizes the response of “oxidation-reduction voltages”. With the help of this measurement, oxidation and reduction voltage range is determined. The number of peaks and the positions typically depend on the material type. [57]. The example of CV curve is seen in Figure 2-7.

The graph of a CV is called voltammogram. In a voltammogram, x axis represents applied potential (E), while y-axis is the response of the applied potential called current [58, 59].

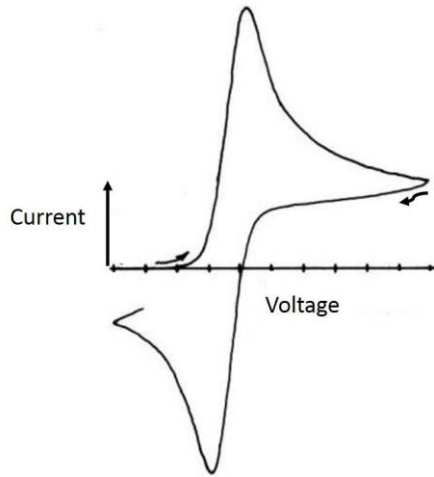


Figure 2-7. Voltammogram example [58] [59].

The Nernst equation is linked to the potential of electrochemical cell ( $E$ ), standard potential of species ( $E_0$ ), and oxidation and reduction reactions at equilibrium. In a Nernst equation,  $R$  is the universal gas constant,  $n$  is the number of electrons and  $T$  is temperature in Kelvin and  $F$  is the Faraday constant.

$$E = E_0 - \left( \frac{RT}{zF} \right) \ln \left( \frac{a_{red}}{a_{ox}} \right)$$

Figure 2-8. Nernst Equation [57, 59].

Above Figure 2-8 is Nernst Equation. The equation provides an insight about the response changes in concentration of the species and the changes in electrode potential. When standard potential is half of the actual potential, the equilibrium will be achieved [57, 60, 61].

#### 2.3.2.2. Electrochemical Impedance Spectroscopy (EIS)

Electrochemical impedance spectroscopy (EIS) is a necessary tool to have a deeper insight about the electrochemical behavior of the materials used for electrochemical purposes. It conducts a systematic analysis of kinetic parameters derived from impedance measurements of positive electrodes [62].

EIS spectra of cathode electrodes are strongly dependent on battery history and testing specifications. The value of the diameter of the semicircle on the Z real axis is almost equal to the charge transfer resistance ( $R_{ct}$ ).

The semicircle at medium characterization and at the high-frequency region, indicates the  $\text{Li}^+$  migration through the surface of film and film capacitance. Also, the semicircle at medium for lower frequencies presents the ion transfer. The straight line in the low-frequency region represents the diffusion of the lithium ions into the bulk of the electrode material also called Warburg diffusion [62-64].

#### 2.3.2.3. Rate Capability

In the midst of physical, chemical and electrochemical characterizations, rate capability tests are one of the most significant electrochemical tests, which required tests fast charge/discharge and high power output for cathode materials, especially for high power density requirements such as automotive applications. Rate capability determines electrochemical capacity at high cycling rates such as high currents [65].

Moreover, it strictly depends on the potential when the cell is being discharged, which are considered large high rates of charge and discharge. The potential which is obtained may depend on various factors other than the active material. The factors might be electrode contact with the current collector, the pressure applied to the electrode and/or shelf life of the component, and homogeneity of the electrode slurry or binding agent of the slurry [66].

#### 2.3.2.4. Charge Discharge Tests

Charge and discharge tests are another type of electrochemical tests. Each battery type has individual conditions and restrictions, which brings different charge and discharge regime. The tests are performed at specific current rates and different cycle numbers [67].

### 3. RESULTS AND DISCUSSION

#### 3.1. NCA Powder Synthesis

##### 3.1.1. XRD Tests

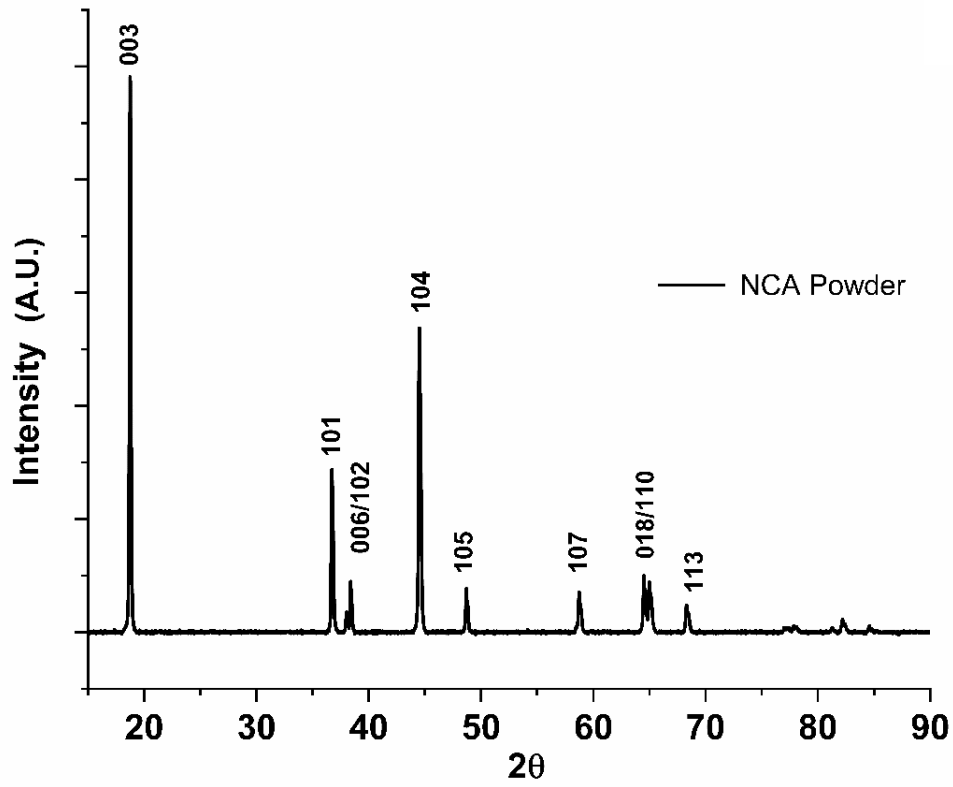


Figure 3-1. XRD Results of NCA Powder.

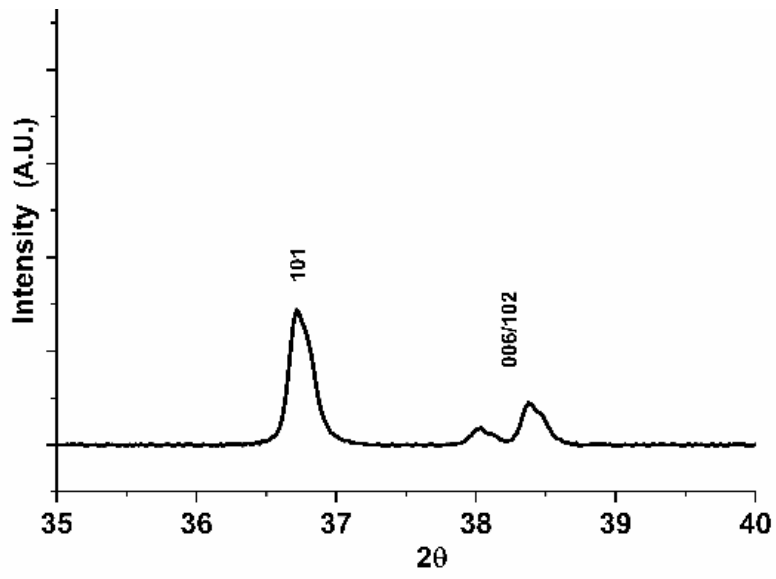


Figure 3-2. 006/102 Double Peak of NCA.

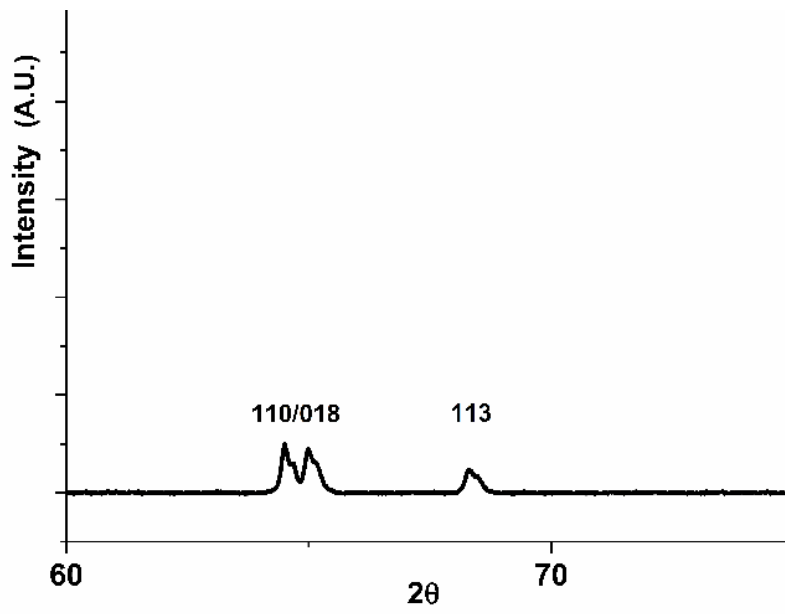


Figure 3-3. 110/018 Double Peaks of NCA.

Table 3-1. Crystallite size of the main peak.

|                              |                   |
|------------------------------|-------------------|
| *                            | <b>Peak 1 003</b> |
| <b>Crystallite size (nm)</b> | 107               |

As shown in Figure 3-1 and 3-2 all the diffraction peaks of NCA can be indexed to fine layered  $\text{Cu K}\alpha$ . While the black line represents the powder version, blue and red spectrums, respectively, indicate Nafion coated and bare NCA electrodes. No variations in pristine electrode were observed in the case of Nafion's presence expect for one peak arising from the carbon electrode itself. In the case of  $\text{Ni}^{+2}$ , ions are easily mixed with  $\text{Li}^{+2}$  ions due to their same ionic radii and these  $\text{Ni}^{+2}$  ions presumably speed the intercalation and deintercalation reactions [16, 27, 33]. Furthermore, inserting the oxidized  $\text{Ni}^{+2}$  into  $\text{Ni}^{+3}$  ions are extremely difficult and the extent of cation mixing in the structure can be estimated from the  $I(003)/I(104)$  (R) intensity ratio. In addition, average crystallite size of NCA particles sintered at  $750\text{ }^\circ\text{C}$  is 9.12 nm. In addition to them, double peaks of powder from Figure 3-2 and 3-3 prove the presence of hexagonal structure which is clearly seen in NCA cathode [68].

### 3.1.2. Scanning Electron Microscopy Tests

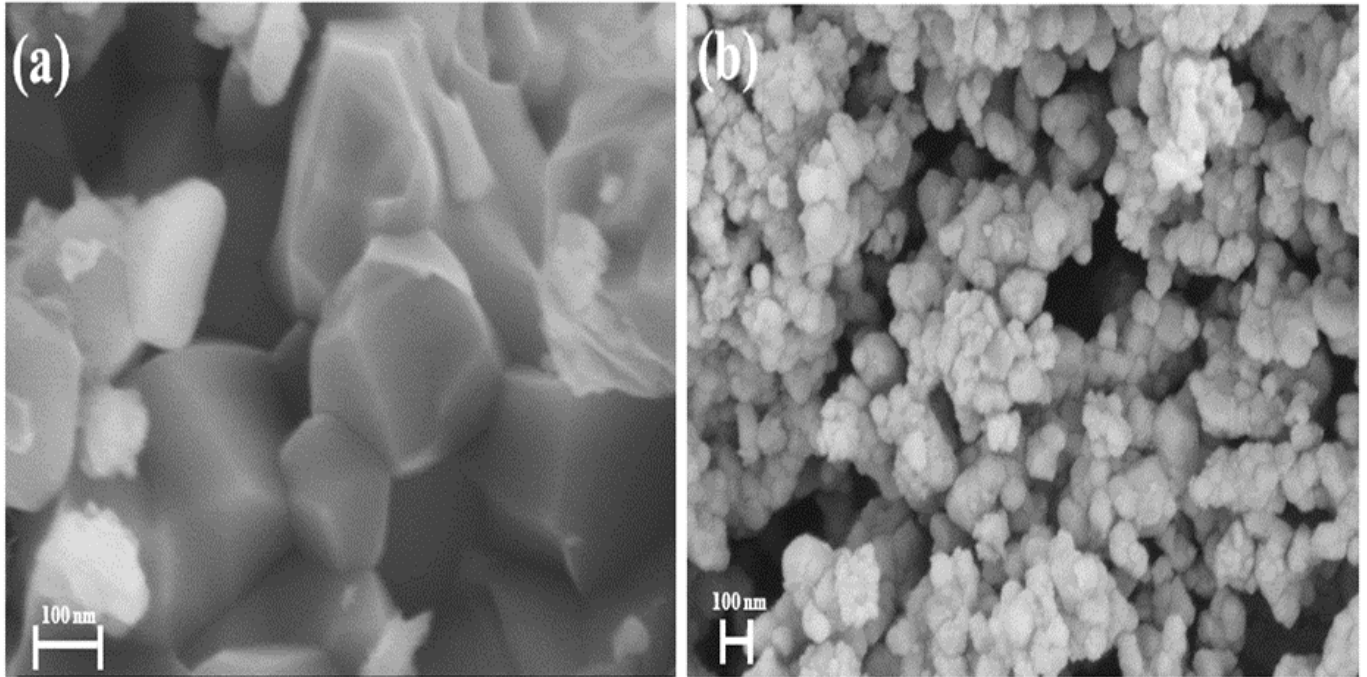


Figure 3-4. SEM Micrograph of NCA Powder.

SEM micrographs of  $\text{LiNi}_{0.80}\text{Co}_{0.15}\text{Al}_{0.05}\text{O}_2$  particles were taken to understand the morphology and detailed structure of the sintered  $\text{LiNi}_{0.80}\text{Co}_{0.15}\text{Al}_{0.05}\text{O}_2$ . NCA powders sintered at  $750^\circ\text{C}$  have particle size of 220 nm and are primary polyhedral in shape.

To differentiate between Nafion coated NCA from the pristine electrode, SEM micrographs were also taken for both electrode surfaces before cycling tests. Figure 3-5 clearly certifies the existing Nafion film on NCA electrode and shows encapsulated NCA powder on the surface of the electrode. The figure also indicates the surface of the pristine NCA electrode on the electrodes are acceptably identical [62, 69]. The size of NCA particles is round 220 nm which is perfectly coherent to the literature findings which are found in references [24, 32].

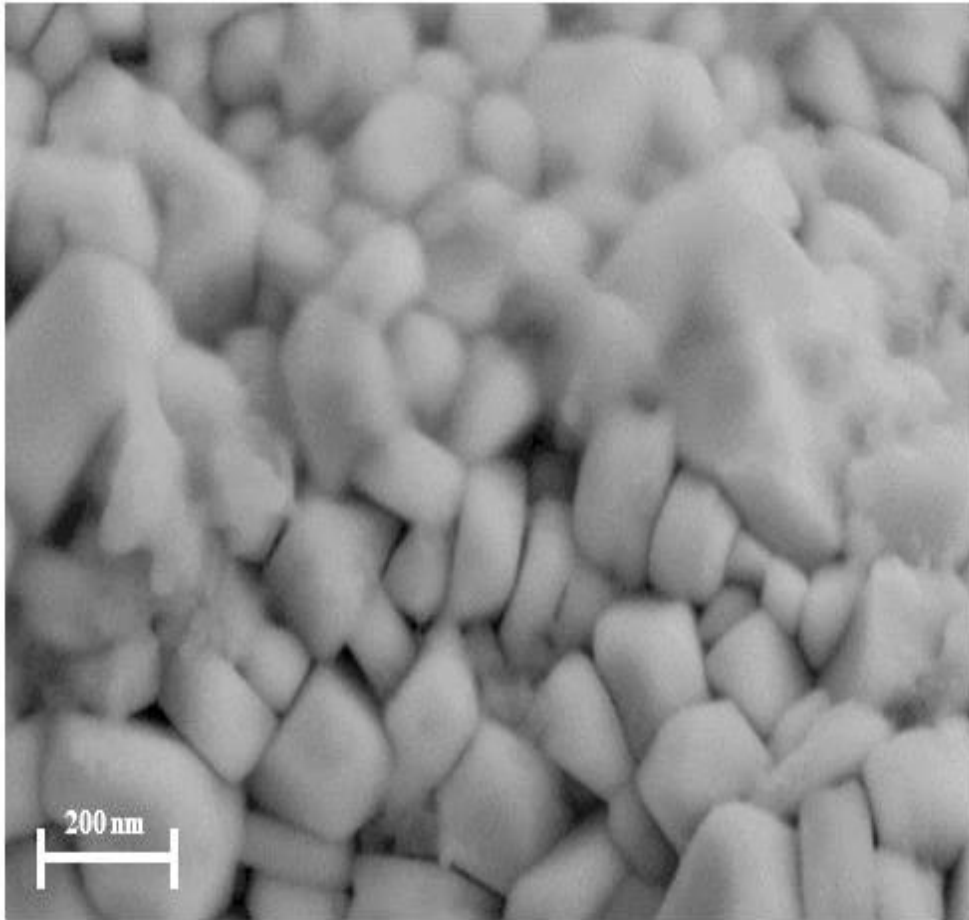


Figure 3-5. Nafion Coated NCA versus Pristine NCA in SEM.

### 3.1.3. Particle Size Distribution

NCA powder size distribution is observed via histogram in Figure 3-6. Image J was used to determine the size of the particles. According to the figure below, while 11 particles are in the range of 0 and 500 nm, the majority of NCA powder is accumulated in between 200 and 300 nm. Also, 11 of NCA particles are found in 0-100 nm range and however there are only 2 particles approximately 427.5 nm in size. The average of the same particles is 240 nm. Even though the structure provides single crystals, multi crystal particles are found as dominate numbers. According to the calculation, 80% of the particles are multi crystalline, while only 20% of them are single crystal.



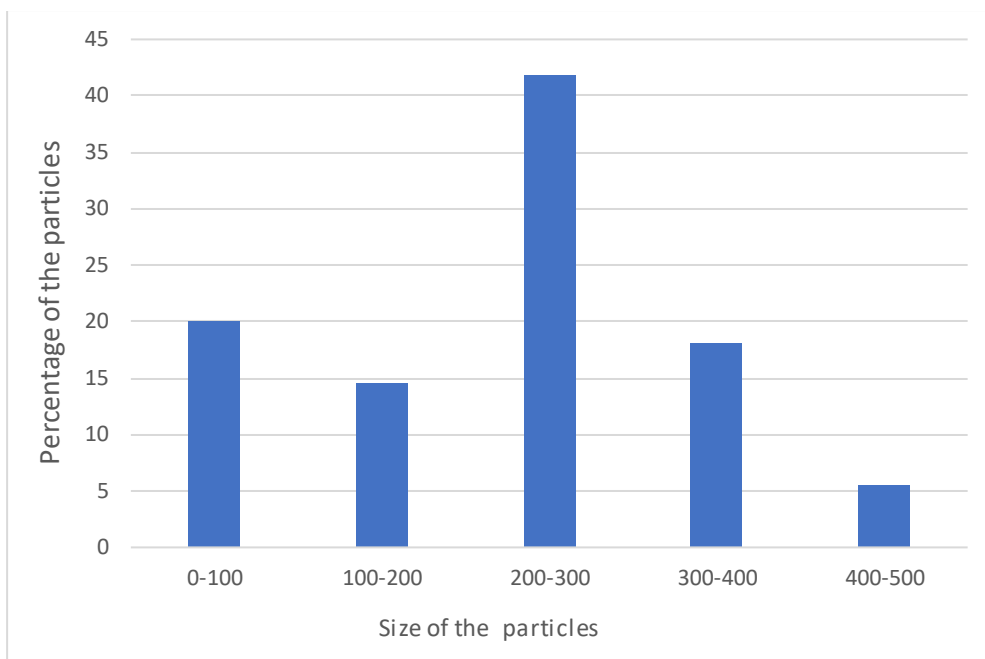


Figure 3-6. Histogram of NCA Powder.

### 3.1.4. Inductively Coupled Plasma Mass Spectroscopy (ICP-MS) Tests

ICP-MS spectroscopy as discussed in the former section detects various elements from ppm to ppb levels for various elements. The certainty of the detection is 50 times higher than ICP-AES which is another similar technique.  $\text{LiNi}_{0.80}\text{Co}_{0.15}\text{Al}_{0.05}\text{O}_2$  powders were analyzed via ICP-MS technique and Table 3-1 presents the percentages of lithium, nickel, cobalt and aluminum oxide for 0.1 g of NCA powder [4, 70].

Table 3.1. ICP-MS spectra.

| Element | %     |
|---------|-------|
| Li      | 8.48  |
| Ni      | 57.54 |
| Co      | 10.63 |

To have a deeper insight into the electrochemical behavior of NCA cathode, the conducted systematic analysis of kinetic parameters was derived from impedance measurements of positive electrodes. EIS spectra of cathode electrodes are strongly

dependent on battery history and testing specifications. The value of the diameter of the semicircle on the Z real axis is almost equal to the charge transfer resistance ( $R_{ct}$ ). Figure 5-1 presents an EIS spectra of battery coin cell as a function of cycle number before cycling. It was clearly seen that there was a marked difference in  $R_{ct}$  after the addition of Nafion (coating). Two of the impedance spectra examined are divided into two different regions [63, 71]. The semicircle at medium characterization at high-frequency region indicates the  $\text{Li}^+$  migration through the surface of film and film capacitance. Also, the semicircle at medium to lower frequencies presents the ion transfer [72]. The straight line in the low-frequency region represents the diffusion of the lithium ions into the bulk of the electrode material which is also called Warburg diffusion [62-64].

### 3.2. Electrochemical Characterization

#### 3.2.1. Cyclic Voltammetry (CV) Test

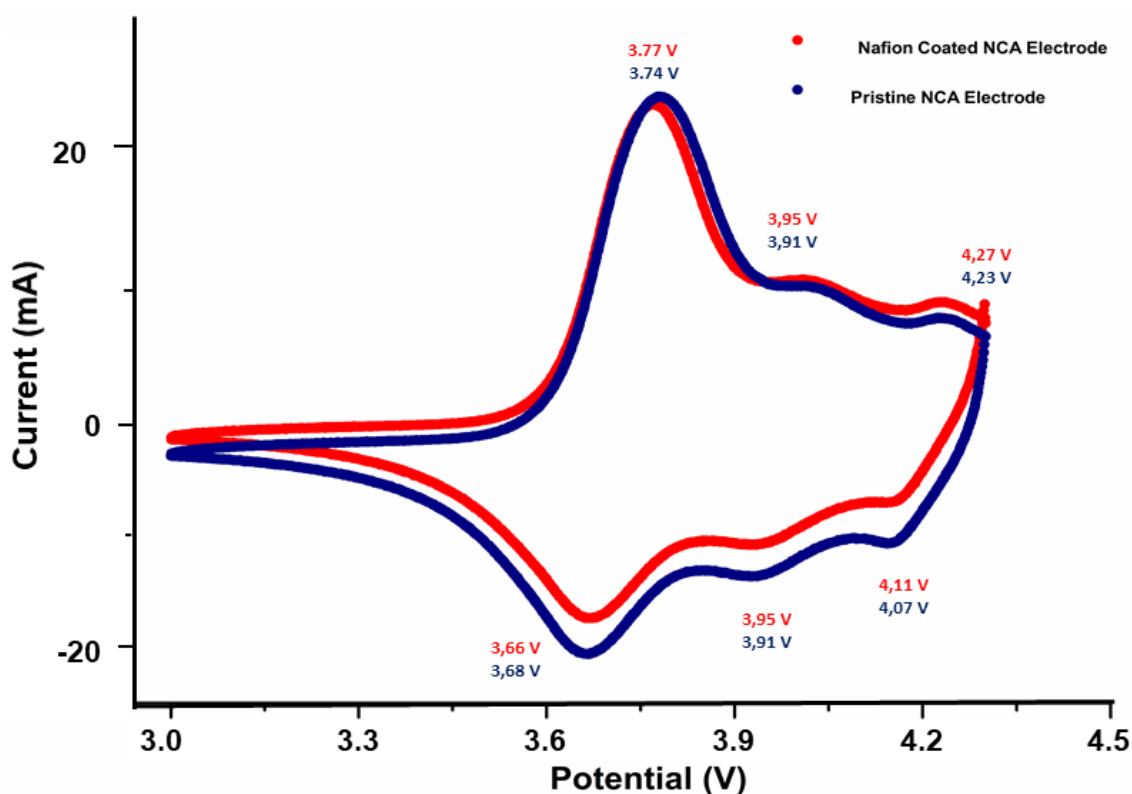


Figure 3-7. Cyclic Voltammograms of Pristine NCA versus Nafion Coated NCA.

Cyclic performance results were conducted at room temperature in the range of 3.0V to 4.2V. The scan rate for the analysis was  $0.05 \text{ mVs}^{-1}$ . Although there was not a strict difference in the peak width and the peak positions among the graphs, peak shifts were observed in Nafion coated NCA cathode. As shown in Figure 3-7 three different

redox couples that correspond to the structural transition occurred during lithium intercalations. That are hexagonal (H2) and from hexagonal to another hexagonal (H3). During these structural transitions, peak shifts were seen in between pristine and Nafion coated NCA electrodes [35].

For instance, while the transition from monoclinic to hexagonal (H2) was seen at 3.77V for Nafion Coated NCA electrode, the same transition was seen at 3.74V for the pristine cathode. Also, pristine NCA is much more severe than that of Nafion coated NCA cathode as it is comparatively shown from the hysteresis differences between oxidation and reduction. Although the differences in peak width and the positions of the peak in hysteresis are not severe, it is suggested that small peak shifts indicate that lithium intercalation and deintercalation process of Nafion coated NCA electrode is more reversible than pristine NCA, that caused the reduction in the polarization of nafion coated NCA cathode. Microcrack formation is the main limiting factor for NCA cathode as it was discussed in the first chapter. This formation occurs from H2 to H3 [73]. Therefore, our modification on NCA cathode is remedy for his microcrack formation. As a result, even though Nafion is not an electrical material, it does not show any voltage. Less polarization may be attributed to the conductivity of NCA [35, 45, 74]. This may also affect the charge and discharge profile under multiple cycles [57].

### **3.2.2. Cyclability Tests**

As it is known from the earlier chapter, the theoretical capacity of NCA is 279 mAh/g. and 80% of this theoretical capacity is reached in practical experiments, since the cathode itself has limitations as have been stated earlier in references [4, 42].

The discharge capacity is around 180 mAh/g in the discharge tests. Although the reached capacity that was achieved in this research was slightly low which is around 19 mAh/g. When compared to similar researches, there is no capacity fade observed in Nafion modified NCA cathode electrode during various discharge tests conducted at different current and voltage rates, which was the aim of this research project. The tests were conducted at different current and voltage tests and the responses were recorded and are reported in Figure 3-8 As seen in the figure, both pristine NCA and Nafion coated NCA were tested in 0.1C, 0.5C , 1C for 100 cycles and 2C for Nafion modified discharge capacity difference was measured as 38 mAh/g. Moreover, there is no capacity fade in Nafion modified NCA electrode. Figure 3-8, 3-9 and Figure 3-10 show the capacity versus voltage for both cells. Even though the capacity differences for both cells are not

high, capability of keeping the current at high voltages are higher in Nafion modified NCA cathode which is seen in overvoltage tests in further section. As seen from the graphs, the capacity for Nafion modified cells are higher than that of the pristine. Even though, discharge capacity for both cells are slightly increasing due to hot press. The percentage of this increasement is severe in Nafion modified cells.

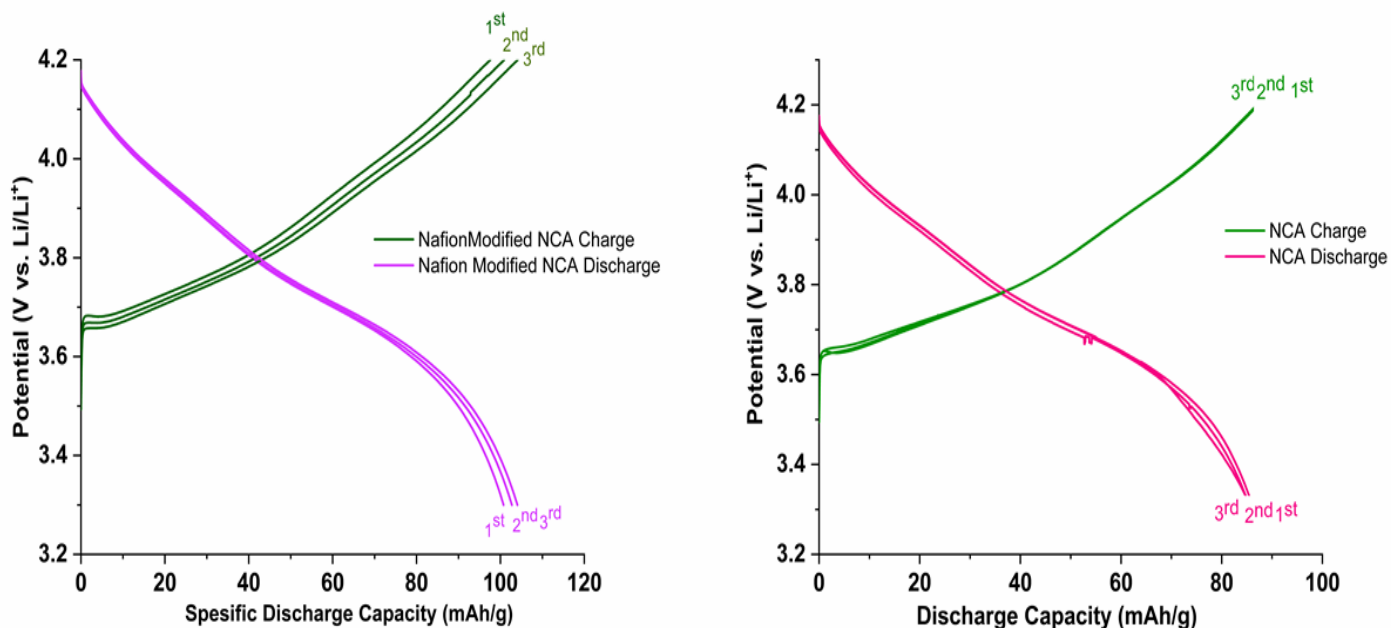


Figure 3-8. Capacity versus Voltage Test of both Electrodes at 0.1C.

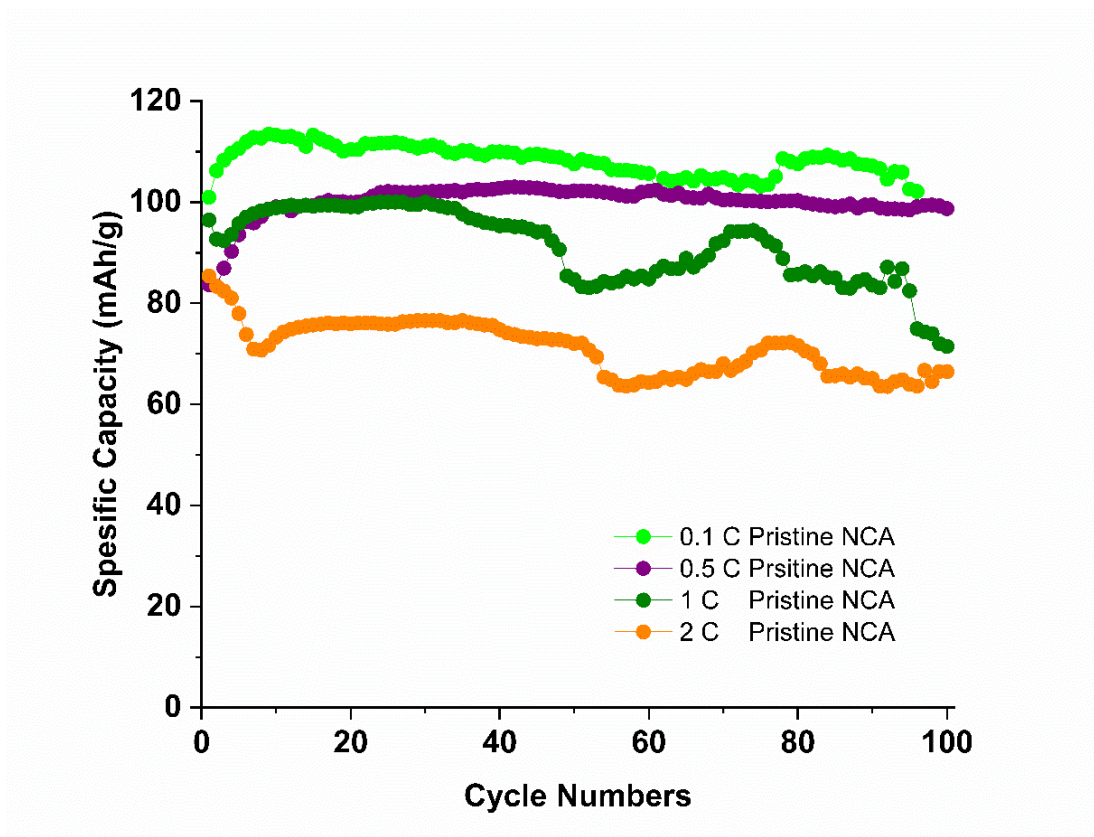


Figure 3-9. Discharge Capacities of Pristine NCA at 0.1C, 0.5C, 1C, 2C for 100 cycles.

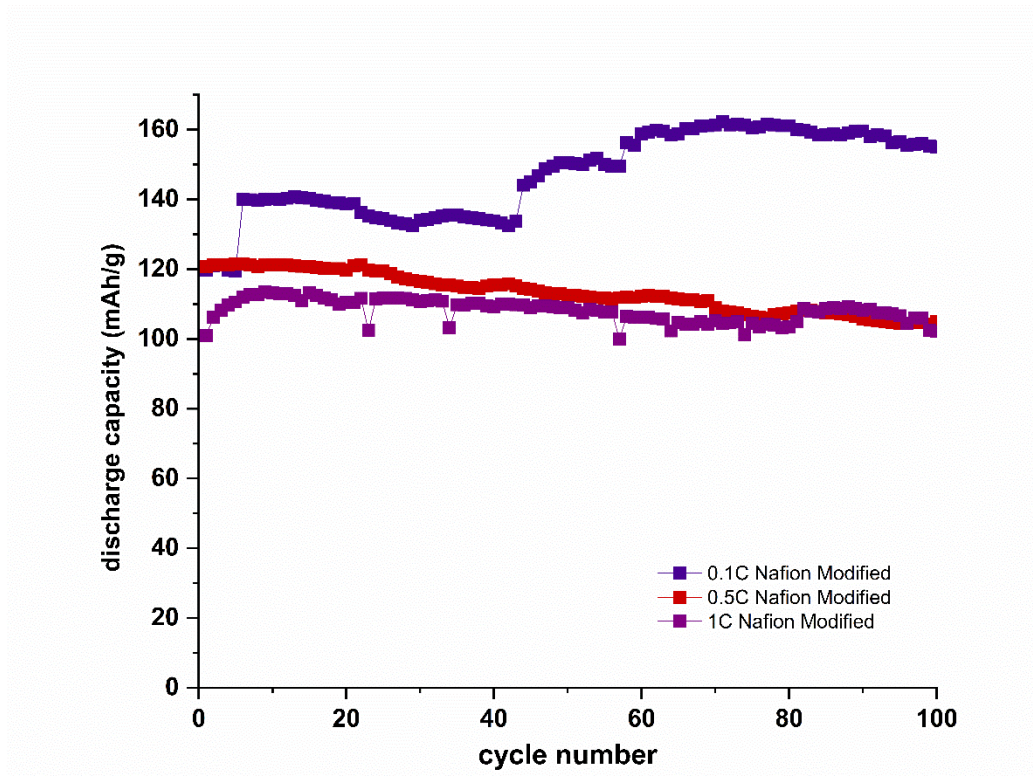


Figure 3-10. Discharge Capacities versus Cycles Numbers for Both Electrodes at 0.1C, 0.5C, 1C for Nafion Modified NCA.

### 3.2.3. Electrochemical Impedance Analysis (EIS) Tests

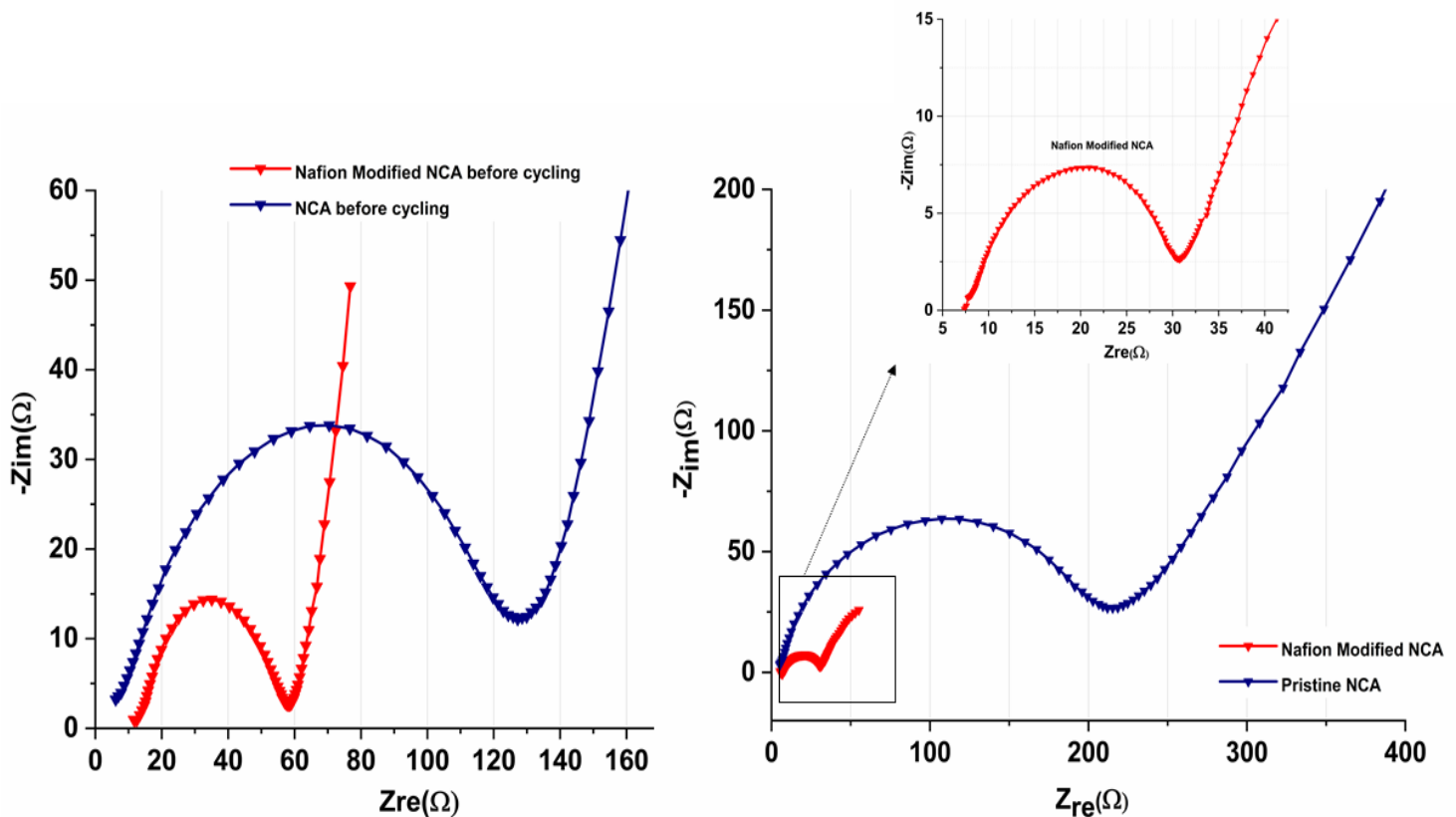


Figure 3-11. EIS spectra of pristine NCA versus Nafion Coated NCA Before Cycling (on the left) and (on the right) EIS spectra of both electrodes.

EIS characterizations imply that both the coin cell batteries have a similar ohmic resistance at the start point of semicircle graph. However, pristine NCA cathode provides a higher semicircle, which can be attributed to a higher charge transfer resistance at the electrode/electrolyte interface. Nafion coated NCA cathode clearly improved easy pathway of  $\text{Li}^+$  insertion and extraction from active material to electrolytic or from electrolyte to active material. Furthermore, Warburg diffusion region shows that Nafion modified NCA has a higher angle of Warburg linear line implying that modified NCA provides a better diffusion of  $\text{Li}^+$  within the electrode [69].

On the other hand, after cycling, Figure 3-11 indicates the evolution of EIS spectra of battery coin cells both for the Nafion-coated and pristine NCA as a function of cycle number after 100 cycles at between 3.3V and 4.2V at 0.1C under open-circuit potentials at 0% DoD. The pristine NCA and Nafion coated NCA cathode have similar ohmic resistance. High-frequency x-axis intersection point of Nafion modified NCA cathode was

observed even before cycling for both the EIS spectra. However, Nafion modified NCA showed two-fold smaller semicircle diameter even after 100 cycles, which depicted the improvement of charge transfer mechanism of both the electrodes. The result is consistent with the increase in specific capacity after 100 cycles.

#### **3.2.4. Rate Capability Tests**

Rate capability test is another significant electrochemical test. Rate capability tests are important to understand the behavior of the battery depending on the different current rates. This test requires fast charge/discharge and/or high power output for cathode materials, especially in high power density requirements such as automotive applications. Rate capability is able to retain electrochemical capacity at high cycling rates such as high currents. It strictly depends on the potential when the cell is in discharge, which is defined as very large at high rates of charge and discharge [75]. The potential which is obtained may depend on various factors other than the active material. These factors might be electrode contact with the current collector, the pressure applied to the electrode and/or shelf life of the component and homogeneity of the electrode slurry or binding agent of the slurry [66].

As seen below in the Figure 3-12, the rate capability tests were conducted for both pristine and Nafion modified NCA cathodes between 3.0V and 4.2V. Both the cells were electrochemically tested. While the pristine NCA cathode's initial discharge capacity was around 115 mAh/g during cycles, the initial discharge capacity of Nafion coated NCA cathode was quite higher, 182 mAh/g. Both cells were galvanostatically charged and discharged starting from 0.1C to 2C. The starting discharge capacity may vary depending on the coating quality. For most of the electrodes, even the type of the coating was the same, initial discharge capacity may have varied between 110-150 mAh/g. Discharge profile for Nafion functionalized cells were reliable even at very high current rates. Furthermore, these cells indicate stable discharge profile during discharge test. Although the discharge capacity was 110 mAh/g for the pristine electrode, the discharge capacity was 182 mAh/g for the Nafion modified NCA cathode. There was 0% capacity fade during tests both for Nafion modified NCA cathode electrode and pristine NCA. Even though the discharge capacity fade for pristine NCA electrode was 0%, the specific discharge profile and the efficiency of the modified cells were more dominant than the pristine cells.



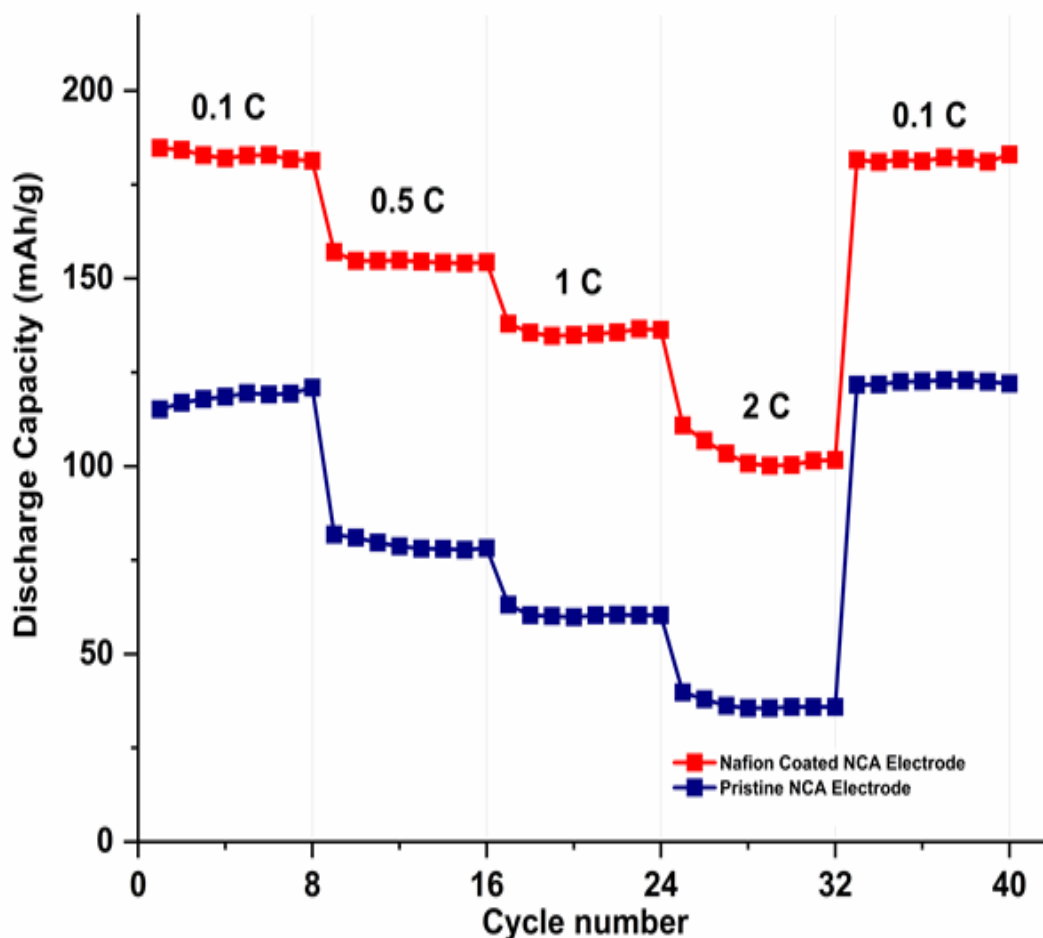


Figure 3-12. Rate Capabilities of NCA and Nafion Modified NCA Cathodes at Different Current Rates.

### 3.2.5. Overvoltage Tests

To understand the responses with increasing the current, both pristine NCA and Nafion modified NCA were subjected to overvoltage tests starting from 4.2C to 4.5C and final voltage range was again the same as the starting voltage which is 4.2V. In literature different discharge voltage ranges are utilized [76]. For example, Watanebe *et al.* have performed NCA battery tests between 2.5 to 4.2V while, Makimura *et al.* have conducted the battery test between 3.0-4.1V for NCA cathode [77]. As indicated in figure 3-13 the overvoltage tests of both pristine and Nafion functionalized NCA is shown for 30 cycles [11, 60, 75, 78, 79]. Even though initial discharge profile up to 4.4V is much more reliable in Nafion film coated NCA, the discharge capacity that are higher than 4.4V is more stable in pristine NCA cathode. Nafion film is decomposed with an increasing voltage, which is higher than 4.4V [29, 79].

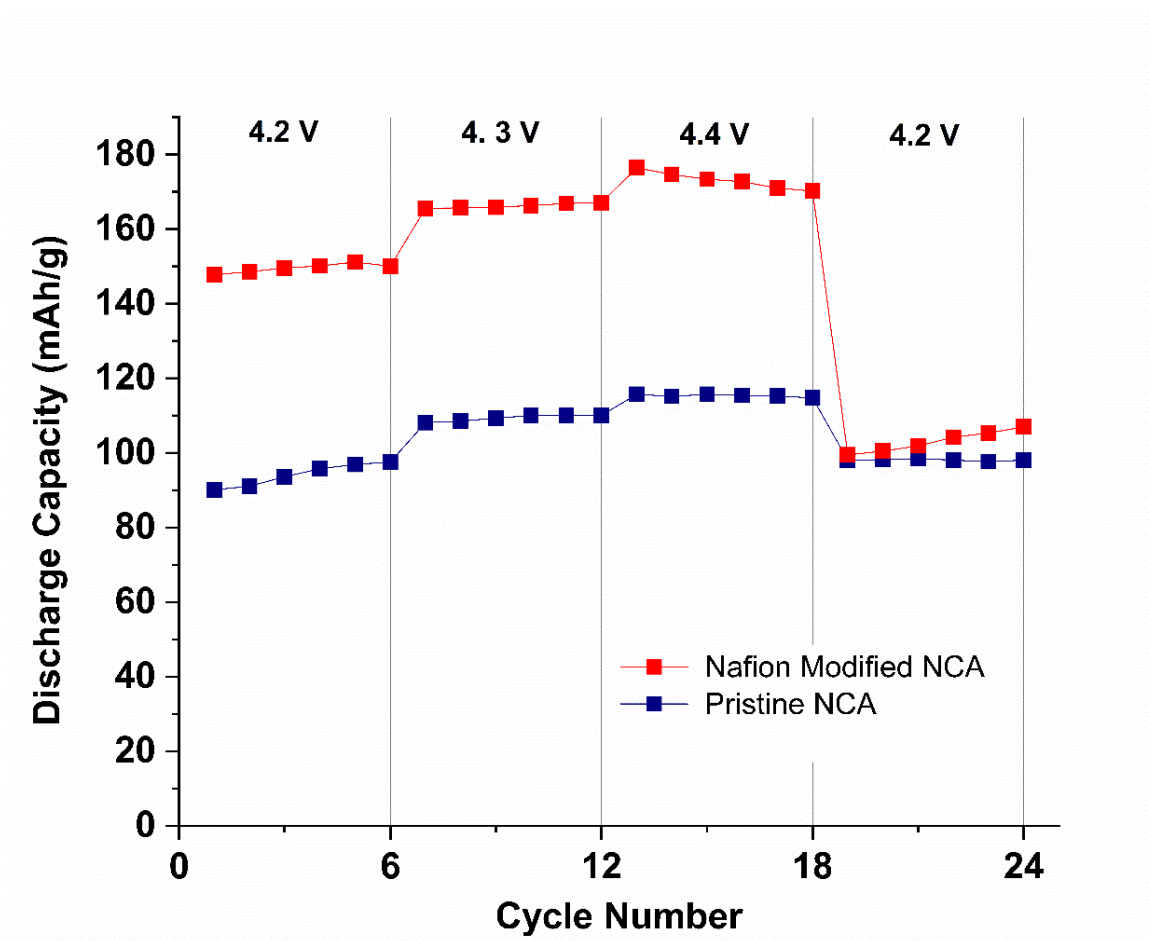


Figure 3-13. Overvoltage Tests of Pristine NCA versus Nafion NCA.

#### 4. CONCLUSION AND FUTURE WORK

*“The important thing is to not stop questioning. Curiosity has its own reason for existence.”*

*Albert Einstein*

In this master thesis, I addressed two major limitations of NCA cathode, which are surface cracks and decomposition of electrolyte under cycling. Both problems cause to decline the capacity during discharge tests and life of the NCA cells. To remedy this problem, the main contribution of our work was the surface modification of NCA cathode done with Nafion thin film. To the best of our knowledge, such surface modification on NCA cathode has never been reported for lithium-ion battery technology.

Synthesized NCA powders were interpreted structurally (XRD, SEM), chemically (ICP-MS) and through electrochemical methods (EIS, CV). According to the obtained results, NCA powders are highly suitable for battery slurry with their higher surface area and excellent crystallite size of 20 nm. After completing these analyses, electrodes were prepared for battery tests. While half of the electrodes were subjected to charge and discharge tests, the other half were coated with Nafion film and then were subjected to the same charge and discharge tests. The battery tests were performed at different current and voltage rates. Tests were comparatively done for two different electrodes (pristine and Nafion coated). All these electrochemical tests indicate that even the initial discharge capacities were close number for both the cells, the differences in the capacity fade during 100 cycles are beyond the estimated values. Although, the initial capacity of pristine NCA cathode was 100.95 mAh/g at 0.1C, and Nafion modified NCA cathode was 155.55 mAh/g at the same current rate. Nafion modified NCA's high current rate was much better than pristine electrodes.

In further work, discharge test of Nafion modified NCA for 100 cycles at 2C will be reported. In the long run, other surface modification of NCA cathode will be further investigated to compare the effect of the electrochemical properties with the surface modification applied in this thesis work. These surface modifications may be combined with each other and the variety of these methods may increase the life and higher cyclability of NCA cells at a reasonable cost.

## 5. APPENDIX

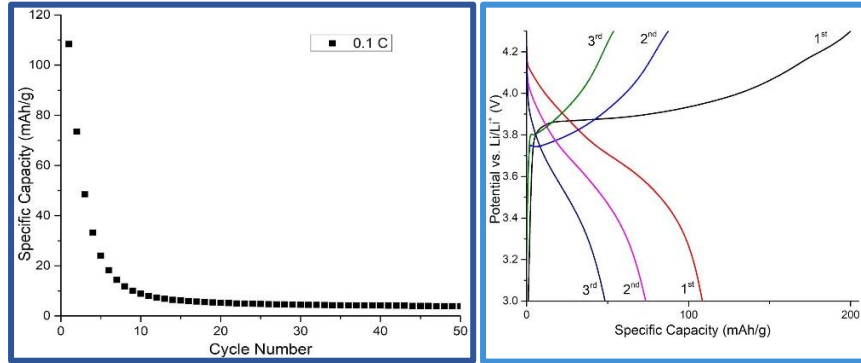


Figure 5-1. (a) Specific Discharge Capacity versus Cycle Number; (b) Capacity versus Voltage of NCA cells.

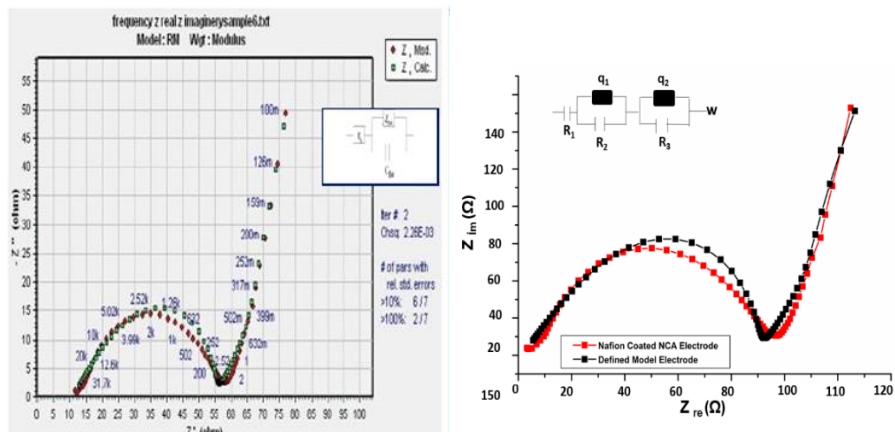


Figure 5-2. Modelling both NCA electrodes in EIS.

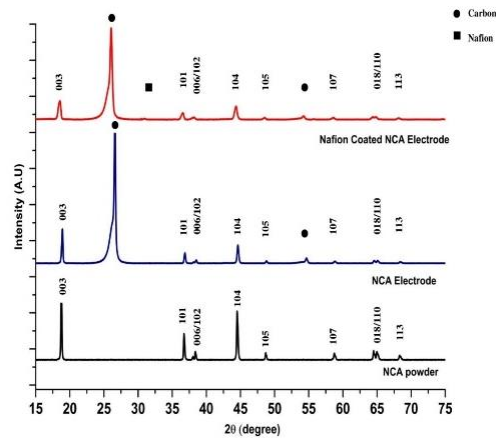


Figure 5-3. XRD of NCA powder and both electrodes.

| Number of Cycle (#) | Specific Charge (mAh/g <sup>1</sup> ) | Number of Cycle (#) | Specific Discharge (mAh/g <sup>1</sup> ) | Number of Cycle (#) | Specific Charge (mAh/g <sup>1</sup> ) | Number of Cycle (#) | Specific Discharge (mAh/g <sup>1</sup> ) |
|---------------------|---------------------------------------|---------------------|--|---------------------|---------------------------------------|---------------------|--|
| 1                   | 210.6                                 | 1                   | 108.5                                    | 1                   | 131.6                                 | 1                   | 75.7                                     |
| 2                   | 97.5                                  | 2                   | 73.5                                     | 2                   | 76.7                                  | 2                   | 71.6                                     |
| 3                   | 62.6                                  | 3                   | 48.4                                     | 3                   | 77.4                                  | 3                   | 71.3                                     |
| 4                   | 41.4                                  | 4                   | 33.2                                     | 4                   | 76.9                                  | 4                   | 73.2                                     |
| 5                   | 28.8                                  | 5                   | 24.0                                     | 5                   | 76.6                                  | 5                   | 73.1                                     |
| 6                   | 21.2                                  | 6                   | 18.2                                     | 6                   | 76.6                                  | 6                   | 73.2                                     |
| 7                   | 16.3                                  | 7                   | 14.4                                     | 7                   | 76.5                                  | 7                   | 74.3                                     |
| 8                   | 13.0                                  | 8                   | 11.9                                     | 8                   | 74.1                                  | 8                   | 75.0                                     |
| 9                   | 10.6                                  | 9                   | 10.0                                     | 9                   | 74.9                                  | 9                   | 74.9                                     |
| 50                  | 1.9                                   | 50                  | 4.0                                      | 23                  | 74.1                                  | 23                  | 74.0                                     |

Figure 5-4. Specific Charge and Discharge Capacity of NCA for Split Cells (left) and for coin cells (right).

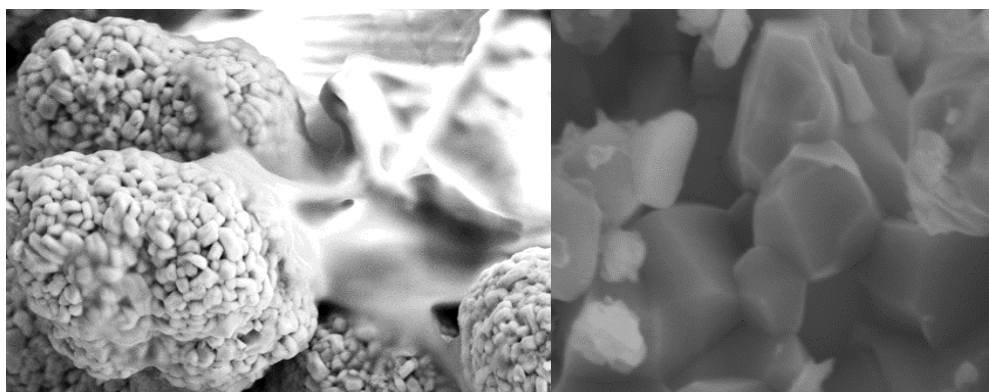


Figure 5-5. Nafion on NCA electrode (left); NCA electrode (right).

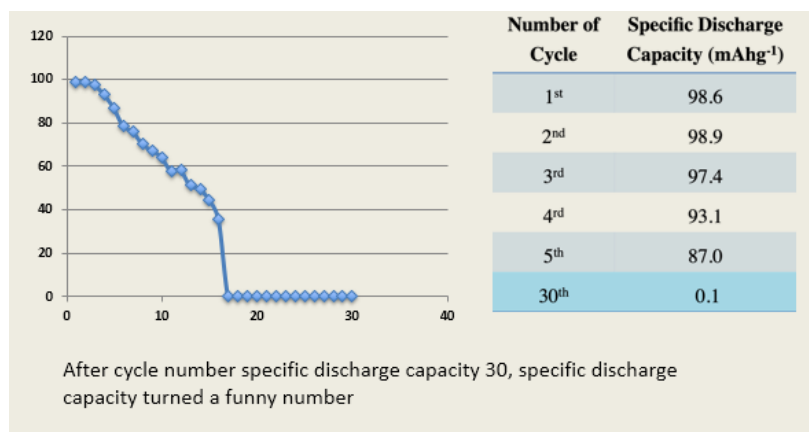


Figure 5-6. Discharge test result of first NCA.

## 6. REFERENCES

1. Brandt, K., *Historical Development of Secondary Lithium Batteries*. Solid State Ionics, 1994. **69**(3-4): p. 173-183.
2. Osiak, M., et al., *Structuring materials for lithium-ion batteries: advancements in nanomaterial structure, composition, and defined assembly on cell performance*. Journal of Materials Chemistry A, 2014. **2**(25): p. 9433-9460.
3. Winter, M. and J.O. Besenhard, *Rechargeable batteries*. Chemie in Unserer Zeit, 1999. **33**(6): p. 320-332.
4. Xu, J., et al., *A review of Ni-based layered oxides for rechargeable Li-ion batteries*. Journal of Materials Chemistry A, 2017. **5**(3): p. 874-901.
5. Nitta, N., et al., *Li-ion battery materials: present and future*. Materials Today, 2015. **18**(5): p. 252-264.
6. Adelhelm, P., M. Armbruster, and F. Kraus, *Solid-State Chemistry 2012*. Nachrichten Aus Der Chemie, 2013. **61**(3): p. 252-264.
7. targray. Battery Separators, 2019, May 7; Available from: <https://www.targray.com/li-ion-battery/separators>.
8. Goodenough, J.B. and Y. Kim, *Challenges for Rechargeable Li Batteries*. Chemistry of Materials, 2010. **22**(3): p. 587-603.
9. 4.7: Ions: Losing and Gaining Electrons. 2018, May 20 Available from: [https://chem.libretexts.org/Courses/College\\_of\\_Marin/Marin%3A\\_CHEM\\_114\\_-\\_Introductory\\_Chemistry\\_\(Daubenmire\)/04%3A\\_Atoms\\_and\\_Elements/4.7%3A\\_Ions%3A\\_Losing\\_and\\_Gaining\\_Electrons](https://chem.libretexts.org/Courses/College_of_Marin/Marin%3A_CHEM_114_-_Introductory_Chemistry_(Daubenmire)/04%3A_Atoms_and_Elements/4.7%3A_Ions%3A_Losing_and_Gaining_Electrons).
10. Lindon, D., *Handbook of Batteries*. 1994, USA: McGraw-Hill.
11. Mehraeen, S., et al., *Homogeneous growth of TiO<sub>2</sub>-based nanotubes on nitrogen-doped reduced graphene oxide and its enhanced performance as a Li-ion battery anode*. Nanotechnology, 2018. **29**(25).

12. Goodenough, J.B., *Cathode materials: A personal perspective*. Journal of Power Sources, 2007. **174**(2): p. 996-1000.
13. Broussely, M. and G. Archdale, *Li-ion batteries and portable power source prospects for the next 5-10 years*. Journal of Power Sources, 2004. **136**(2): p. 386-394.
14. Lindon, D., *handbook of batteries*
15. Ellis, B.L., K.T. Lee, and L.F. Nazar, *Positive Electrode Materials for Li-Ion and Li-Batteries*. Chemistry of Materials, 2010. **22**(3): p. 691-714.
16. Yao, W.J., et al., *Na<sub>2</sub>Fe(C<sub>2</sub>O<sub>4</sub>)F-2: A New Iron-Based Polyoxyanion Cathode for Li/Na Ion Batteries*. Chemistry of Materials, 2017. **29**(5): p. 2167-2172.
17. Chung, S.Y., *Comment on "Positive Electrode Materials for Li-Ion and Li-Batteries"*. Chemistry of Materials, 2012. **24**(11): p. 2240-2243.
18. Fischer, J., et al., *Structural transformation of sputtered o-LiMnO<sub>2</sub> thin-film cathodes induced by electrochemical cycling*. Thin Solid Films, 2013. **549**: p. 263-267.
19. Jang, Y.I., et al., *Electrochemical cycling-induced spinel formation in high-charge-capacity orthorhombic LiMnO<sub>2</sub>*. Journal of the Electrochemical Society, 1999. **146**(9): p. 3217-3223.
20. Zhu, C.Y., et al., *Achieving High-Performance Silicon Anodes of Lithium-Ion Batteries via Atomic and Molecular Layer Deposited Surface Coatings: an Overview*. Electrochimica Acta, 2017. **251**: p. 710-728.
21. Daniel, C., et al., *Cathode Materials Review*. Review on Electrochemical Storage Materials and Technology, 2014. **1597**: p. 26-43.
22. Kim, J., et al., *Prospect and Reality of Ni-Rich Cathode for Commercialization*. Advanced Energy Materials, 2018. **8**(6).
23. Konstantinov, K., et al., *Stoichiometry-controlled high-performance LiCoO<sub>2</sub> electrode materials prepared by a spray solution technique*. Journal of Power Sources, 2003. **119**: p. 195-200.
24. Leifer, N., et al., *LiNi<sub>0.8</sub>Co<sub>0.15</sub>Al<sub>0.05</sub>O<sub>2</sub> Cathode Material: New Insights via Li-7 and Al-27 Magic-Angle Spinning NMR Spectroscopy*. Chemistry of Materials, 2016. **28**(21): p. 7594-7604.
25. Liu, Z.H., et al., *Modification of LiNi<sub>0.8</sub>Co<sub>0.15</sub>Al<sub>0.05</sub>O<sub>2</sub> using nanoscale carbon coating*. Journal of Alloys and Compounds, 2018. **763**: p. 701-710.
26. Mekonnen, Y., A. Sundararajan, and A.I. Sarwat, *A Review of Cathode and Anode Materials for Lithium-Ion Batteries*. Southeastcon 2016, 2016.
27. Sun, S.W., et al., *Surface-modified Li[Li<sub>0.2</sub>Ni<sub>0.17</sub>Co<sub>0.07</sub>Mn<sub>0.56</sub>]O<sub>2</sub> nanoparticles with MgF<sub>2</sub> as cathode for Li-ion battery*. Solid State Ionics, 2015. **278**: p. 85-90.
28. Song, C.H., et al., *Improving the Electrochemical Performance of LiNi<sub>0.80</sub>Co<sub>0.15</sub>Al<sub>0.05</sub>O<sub>2</sub> in Lithium Ion Batteries by LiAlO<sub>2</sub> Surface Modification*. Applied Sciences-Basel, 2018. **8**(3).

29. Chen, T., et al., *The effect of gradient boracic polyanion-doping on structure, morphology, and cycling performance of Ni-rich LiNi<sub>0.8</sub>Co<sub>0.15</sub>Al<sub>0.05</sub>O<sub>2</sub> cathode material (vol 374, pg 1, 2018)*. Journal of Power Sources, 2018. **392**: p. 296-296.
30. Wang, Q.S., et al., *A review of lithium ion battery failure mechanisms and fire prevention strategies*. Progress in Energy and Combustion Science, 2019. **73**: p. 95-131.
31. Purwanto, A., et al., *NCA cathode material: synthesis methods and performance enhancement efforts*. Materials Research Express, 2018. **5**(12).
32. Liu, W.M., et al., *Green and low-cost synthesis of LiNi<sub>0.8</sub>Co<sub>0.15</sub>Al<sub>0.05</sub>O<sub>2</sub> cathode material for Li-ion*. Materials Letters, 2019. **246**: p. 153-156.
33. Tang, A.D., et al., *Layered Li-Ni-Co-Mn-O as cathode materials for lithium ion battery*. Progress in Chemistry, 2007. **19**(9): p. 1313-1321.
34. Meng, F., et al., *Modification of Li [Li<sub>0.2</sub>Mn<sub>0.54</sub>Ni<sub>0.13</sub>Co<sub>0.13</sub>] O<sub>2</sub> cathode with  $\alpha$ -MoO<sub>3</sub> via a simple wet chemical coating process*. Applied Surface Science, 2019.
35. Park, T.J., J.B. Lim, and J.T. Son, *Effect of Calcination Temperature of Size Controlled Microstructure of LiNi<sub>0.8</sub>Co<sub>0.15</sub>Al<sub>0.05</sub>O<sub>2</sub> Cathode for Rechargeable Lithium Battery*. Bulletin of the Korean Chemical Society, 2014. **35**(2): p. 357-364.
36. Chen, T., et al., *The effect of gradient boracic polyanion-doping on structure, morphology, and cycling performance of Ni-rich LiNi<sub>0.8</sub>Co<sub>0.15</sub>Al<sub>0.05</sub>O<sub>2</sub> cathode material*. Journal of Power Sources, 2018. **374**: p. 1-11.
37. Kalantarian, M.M., S. Asgari, and P. Mustarelli, *A theoretical approach to evaluate the rate capability of Li-ion battery cathode materials*. Journal of Materials Chemistry A, 2014. **2**(1): p. 107-115.
38. Zhou, H.M., et al., *An electrolyte to improve the deep charge-discharge performance of LiNi<sub>0.8</sub>Co<sub>0.15</sub>Al<sub>0.05</sub>O<sub>2</sub> cathode*. Journal of Materials Science-Materials in Electronics, 2018. **29**(8): p. 6648-6659.
39. Nair, N.K.C. and N. Garimella, *Battery energy storage systems: Assessment for small-scale renewable energy integration*. Energy and Buildings, 2010. **42**(11): p. 2124-2130.
40. Ju, S.H., J.H. Kim, and Y.C. Kang, *Electrochemical properties of LiNi<sub>0.8</sub>Co<sub>0.2-x</sub>Al<sub>x</sub>O<sub>2</sub> (0 ≤ x ≤ 0.1) cathode particles prepared by spray pyrolysis from the spray solutions with and without organic additives*. Metals and Materials International, 2010. **16**(2): p. 299-303.
41. Kalyani, P. and N. Kalaiselvi, *Various aspects of LiNiO<sub>2</sub> chemistry: A review*. Science and Technology of Advanced Materials, 2005. **6**(6): p. 689-703.
42. Kumar, P.S., et al., *Preparation and characterization of LiNi<sub>0.495</sub>M<sub>0.01</sub>Mn<sub>0.495</sub>O<sub>2</sub> (M = Zn, Co, and Y) for lithium ion batteries*. Ionics, 2017. **23**(11): p. 3013-3022.
43. Chung, Y., et al., *A Surfactant-based Method for Carbon Coating of LiNi<sub>0.8</sub>Co<sub>0.15</sub>Al<sub>0.05</sub>O<sub>2</sub> Cathode in Li Ion Batteries*. Bulletin of the Korean Chemical Society, 2010. **31**(8): p. 2304-2308.



44. Kim, Y., *Encapsulation of LiNi<sub>0.5</sub>Co<sub>0.2</sub>Mn<sub>0.3</sub>O<sub>2</sub> with a thin inorganic electrolyte film to reduce gas evolution in the application of lithium ion batteries*. Physical Chemistry Chemical Physics, 2013. **15**(17): p. 6400-6405.
45. Shim, J.H., et al., *Reduced Graphene Oxide-Wrapped Nickel-Rich Cathode Materials for Lithium Ion Batteries*. ACS Applied Materials & Interfaces, 2017. **9**(22): p. 18720-18729.
46. Eyovge, C. and T. Ozturk, *Nafion Coated Mg<sub>50</sub>Ni<sub>50</sub> and (La,Mg)<sub>2</sub>Ni<sub>7</sub> Negative Electrodes for NiMH Batteries*. Journal of the Electrochemical Society, 2018. **165**(10): p. A2203-A2208.
47. Brandon D, W.D.K., *Diffraction Analysis of Crstal Structure* Microstructural Characterization of Materials 2008: p. 57-20.
48. Chemisty, R.S.o., *Powder Difrraction Theory and Practice*. 2008.
49. Tayyar, B., *Hacettepe University Department of Chemcial Engineering XRD in theory and practice*. p. <http://yunus.hacettepe.edu.tr/~selis/teaching/WEBkmu396/ppt/Presentations2010/XRD.pdf>.
50. Stock, B.D.C.a.S.R., *Elements of X-ray Difrraction* 2001. **3 edition**.
51. Mourao, R.L., et al., *TEM/SEM morphological analysis of dental tissue-resin bonding system in dry and wet conditions*. Bioceramics 15, 2003. **240-2**: p. 357-360.
52. Leimer, *Scanning Electron Microscopy Physics of Image Formation and Microanalysis*. Vol. 45. Springer.
53. Marturi, N., S. Dembele, and N. Piat, *Depth and Shape Estimation from Focus in Scanning Electron Microscope for Micromanipulation*. 2013 International Conference on Control, Automation, Robotics and Embedded Systems (Care-2013), 2013.
54. Rao, R.N. and M.V.N.K. Talluri, *An overview of recent applications of inductively coupled plasma-mass spectrometry (ICP-MS) in determination of inorganic impurities in drugs and pharmaceuticals*. Journal of Pharmaceutical and Biomedical Analysis, 2007. **43**(1): p. 1-13.
55. Wen, F., et al., *Graphene-embedded LiMn<sub>0.8</sub>Fe<sub>0.2</sub>PO<sub>4</sub> composites with promoted electrochemical performance for lithium ion batteries*. Electrochimica Acta, 2018. **276**: p. 134-141.
56. Yang, S., et al., *Electrochemical and Electronic Charge Transport Properties of Ni-Doped LiMn<sub>2</sub>O<sub>4</sub> Spinel Obtained from Polyol-Mediated Synthesis*. Materials, 2018. **11**(5).
57. Hendel, S.J. and E.R. Young, *Introduction to Electrochemistry and the Use of Electrochemistry to Synthesize and Evaluate Catalysts for Water Oxidation and Reduction*. Journal of Chemical Education, 2016. **93**(11): p. 1951-1956.
58. Connelly, N.G. and W.E. Geiger, *Chemical redox agents for organometallic chemistry*. Chemical Reviews, 1996. **96**(2): p. 877-910.
59. Elgrishi, N., et al., *A Practical Beginner's Guide to Cyclic Voltammetry*. Journal of Chemical Education, 2018. **95**(2): p. 197-206.

60. Aguilo-Aguayo, N. and T. Bechtold, *Monitoring the State-of-Charge in All-Iron Aqueous Redox Flow Batteries*. Journal of the Electrochemical Society, 2018. **165**(13): p. A3164-A3168.
61. Biesheuvel, P.M., Y. Fu, and M.Z. Bazant, *Electrochemistry and capacitive charging of porous electrodes in asymmetric multicomponent electrolytes*. Russian Journal of Electrochemistry, 2012. **48**(6): p. 580-592.
62. Gantenbein, S., M. Weiss, and E. Ivers-Tiffée, *Impedance based time-domain modeling of lithium-ion batteries: Part I*. Journal of Power Sources, 2018. **379**: p. 317-327.
63. Shenouda, A.Y. and A.A. Momchilov, *A study on graphene/tin oxide performance as negative electrode compound for lithium battery application*. Journal of Materials Science-Materials in Electronics, 2019. **30**(1): p. 79-90.
64. Eliseeva, S.N., et al., *Electrochemical impedance spectroscopy characterization of LiFePO<sub>4</sub> cathode material with carboxymethylcellulose and poly-3,4-ethylendioxythiophene/polystyrene sulfonate*. Electrochimica Acta, 2017. **227**: p. 357-366.
65. An, F.Q., et al., *Rate dependence of cell-to-cell variations of lithium-ion cells*. Scientific Reports, 2016. **6**.
66. Qi, Z.X. and G.M. Koenig, *Electrochemical Evaluation of Suspensions of Lithium-Ion Battery Active Materials as an Indicator of Rate Capability*. Journal of the Electrochemical Society, 2017. **164**(2): p. A151-A155.
67. Raccichini, R., M. Amores, and G. Hinds, *Critical Review of the Use of Reference Electrodes in Li-Ion Batteries: A Diagnostic Perspective*. Batteries-Basel, 2019. **5**(1).
68. Ozden, A., et al., *Enhancement of direct methanol fuel cell performance through the inclusion of zirconium phosphate*. International Journal of Hydrogen Energy, 2017. **42**(33): p. 21501-21517.
69. Rubinson, J.F. and Y.P. Kayinamura, *Charge transport in conducting polymers: insights from impedance spectroscopy*. Chemical Society Reviews, 2009. **38**(12): p. 3339-3347.
70. Tan, S., et al., *Recent Progress in Research on High-Voltage Electrolytes for Lithium-Ion Batteries*. Chemphyschem, 2014. **15**(10): p. 1956-1969.
71. Schmidt, J.P., et al., *Studies on LiFePO<sub>4</sub> as cathode material using impedance spectroscopy*. Journal of Power Sources, 2011. **196**(12): p. 5342-5348.
72. Zhou, X., et al., *Impedance characterization of lithium-ion batteries aging under high-temperature cycling: Importance of electrolyte-phase diffusion*. Journal of Power Sources, 2019. **426**: p. 216-222.
73. Xu, J., et al., *Understanding the Degradation Mechanism of Lithium Nickel Oxide Cathodes for Li-Ion Batteries*. Acs Applied Materials & Interfaces, 2016. **8**(46): p. 31677-31683.
74. Oh, S.J., J.K. Lee, and W.Y. Yoon, *Preventing the Dissolution of Lithium Polysulfides in Lithium-Sulfur Cells by using Nafion-coated Cathodes*. Chemsuschem, 2014. **7**(9): p. 2562-2566.

75. Shen, Y., D. Noreus, and S. Starborg, *Increasing NiMH battery cycle life with oxygen*. International Journal of Hydrogen Energy, 2018. **43**(40): p. 18626-18631.
76. Watanabe, S., et al., *Capacity fade of LiAl<sub>y</sub>Ni<sub>1-x-y</sub>Co<sub>x</sub>O<sub>2</sub> cathode for lithium-ion batteries during accelerated calendar and cycle life tests (surface analysis of LiAl<sub>y</sub>Ni<sub>1-x-y</sub>Co<sub>x</sub>O<sub>2</sub> cathode after cycle tests in restricted depth of discharge ranges)*. Journal of Power Sources, 2014. **258**: p. 210-217.
77. Makimura, Y., et al., *Factors affecting cycling life of LiNi<sub>0.8</sub>Co<sub>0.15</sub>Al<sub>0.05</sub>O<sub>2</sub> for lithium-ion batteries*. Journal of Materials Chemistry A, 2016. **4**(21): p. 8350-8358.
78. Adams, K., et al., *Facile synthesis and characterization of Bi<sub>13</sub>S<sub>18</sub>I<sub>2</sub> films as a stable supercapacitor electrode material*. Journal of Materials Chemistry A, 2019. **7**(4): p. 1638-1646.
79. Ye, Z., D. Noreus, and J.R. Howlett, *Metal hydrides for high-power batteries*. Mrs Bulletin, 2013. **38**(6): p. 504-508.